STEADY STATE SIMULATION OF FORCED CIRCULATION EVAPORATION

A Thesis Submitted
In Partial Fulfilment of the Requirements
for the Degree of
MASTER OF TECHNOLOGY

By
PARESH CHANDRA DAS

to the
DEPARTMENT OF CHEMICAL ENGINEERING
INDIAN INSTITUTE OF TECHNOLOGY, KANPUR
JANUARY, 1979

I.I.T. KANPUR
CENTRAL LIBRARY
Acc. No. 58350
12 APR 1979
CHE-1979-M-DAS-STE

CERTIFICATE

This is to certify that the present work, 'STEADY STATE SIMULATION OF FORCED CIRCULATION EVAPORATION' has been carried out under my supervision and has not been submitted elsewhere for a degree.

Date: January 23, 1979

(Dr.) H. Veeramani
Assistant Professor
Department of Chemical Engineering
Indian Institute of Technology
Kanpur-208016, India

POST GRADUATE OFFICE
This thesis has been approved for the award of the Degree of Master of Technology (M.Tech.) in accordance with the regulations of the Indian Institute of Technology Kanpur
Dated. 12.3.79

ACKNOWLEDGEMENTS

The author of this thesis wishes to express his gratitude to Dr. H. Veeramani for establishing the type of student-professor relationship which allowed the most latitude on the author's development of this work. His conception of the topic and all the helpful hints he provided contributed greatly to the successful development of this thesis, without being an overbearing influence.

IIT-Kanpur Computer Centre has provided a number of personnel who have been a great aid in author's endeavors. Special mention goes to Computer Operator Mr. V.S. Seal for his favor.

The author sincerely acknowledges help rendered by Mr.Ramnath in proof reading the manuscript.

The author is indebted to numerous friends and colleagues for their constant encouragement. Special mention goes to Mr. R.M. Kakwani and Mr. Ramnath.

Last but not least, author thanks Mr. B.S. Pandey for his untiring help in typing the thesis, and Mr. Panesar in preparing the drawings.

Author

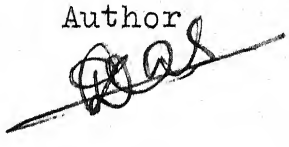

CONTENTS

CHAPTER

LIST OF FIGURES

LIST OF TABLES

ABSTRACT

A mathematical model has been developed for simulation of forced circulation evaporation process. Computer programme written in FORTRAN, based on the mathematical model predicts the performance of forced circulation evaporator for variation in operational parameters like feed rate, feed temperature, concentration of feed liquor and recycle ratio. Mathematical model predicts various quantities like temperature, pressure, pressure gradient, tube side film coefficient, overall heat transfer coefficient, liquor concentration, void fraction at each point along the tube length. Overall performance is determined by integrating the longitudinal profiles. Mathematical model developed is based on basic continuity, momentum, and energy balance equations applied to differential segments of the tube. Along with basic balance equations, different correlations for pressure drop and heat transfer coefficients for the non-boiling and boiling zones have been used in the model. Correlations for engineering properties of black liquor, considered as process liquor, are available from earlier work.

Due to lack of suitable plant data, model was tested on Badger's experimental data on vaporization of water in long vertical tube. The model was found to predict Badger's result satisfactorily. Model was used to study the performance of forced circulation evaporation in a single vertical tube,

and in a three pass unit with single tube per pass for both vertical and horizontal orientation of calendria. Bamboo and Bagasse black liquors were considered to illustrate the effect of viscosity on the performance of forced circulation evaporator.

NOMENCLATURE

A	Cross sectional area of tube, m^2
C	Specific heat, kcal/kg ^oC
D	Tube diameter, m
g	Gravitational acceleration, m/s^2
g_c	Conversion factor, 9.8 $kg.m/kg_f s^2$
G	Mass flux, kg/m^2
h	Heat transfer coefficient, kW/m^2 K
J	Mechanical equivalent of heat, 2091.58 m kg_f/kcal
k	Thermal conductivity, kcal/hr m ^oC
L	Tube length, m
P	Pressure, kg_f/m^2
$\frac{dP}{dz}$	Pressure gradient, kg_f/m^3
Q	Heat flux, kcal/hr m^2
S'	Solid concentration of fresh feed plus recycle
S	Solid concentration, mass fraction
S_e	Solid concentration at the exit of tube
T	Temperature, ^oC
u	Velocity, m/s
U	Overall heat transfer coefficiemt, kW/m^2 K
x	Quality of vapor liquid mixture, fraction
z	Tube length, m
R	Recycle ratio
n	Number of tubes
N	Number of passes
E	Evaporation Rate kg/h

Greek Letters

μ	Viscosity, cp
ρ	Density, kg/m^3
α	Void fraction
λ	Heat of vaporization, kcal/kg
τ	Shear stress, kg_f/m^2

Subscripts

i	Inside, Inlet
o	Outside, outlet, overall
S	Steam
s	Surface
w	Wall
L,F	liquid
v,V	vapor
T	Total
b	Boiling
nb	Non-boiling
f	friction
a	acceleration
e	elevation

CHAPTER 1

INTRODUCTION

Evaporation is an important chemical engineering operation used for concentrating solutions in diverse applications in chemical, food, pharmaceutical and related industries. A summary of the general features of some of the more popular types of evaporators is given in Table 1.1. Forced circulation evaporators (FCE) find applications in concentrating moderately viscous solutions (80-100 cp) with tendencies for solid separation and/or scale formation. Typical process applications of FCE include evaporation of salt brines, electrolytic caustic solutions, black liquor, aluminate liquor etc.

The heating element (calendria) of a FCE is essentially a multipass (2-6 passes) shell and tube heat exchanger and the heated process liquor is flashed in a separator. The desired increase in concentration of the liquors is obtained by recirculating the liquor after flashing. Liquor velocity in the calendria tubes is maintained at 1-6 m/s with a centrifugal pump. Calendria can be positioned vertically or horizontally depending upon space availability and maintenance considerations. Figure 1.1 and Figure 1.2 [27] give schematic sketches of FCE with vertical and horizontal calendria, respectively.

TABLE 1.1: GENERAL FEATURES OF EVAPORATORS USED IN CHEMICAL PROCESS INDUSTRIES

Feature	SE	LTVE	FFE	FCE	ATFE
Orientation	Vert.	Vert.	Vert	Vert/Hor.	Vert/Hor.
Tube length, m	1-2	6-12	2-10	2-7	2-6
Tube dia.,mm	25-50	25-50	25-50	25-50	300-2000
Liquor Recirculation	NO	NO	NO	YES	NO
Limiting viscosity,cp	50	15	50	80-100	3000 p
U,value $kW/m^2{}^oK$	0.8-2.8	1-3.4	0.6-1.7	2-11	Variable[a]
Applications: scaling liq.	NO	YES	NO	YES	YES
Heat sensitive liquor	NO	NO	YES	NO	YES
Foaming liquor	NO	YES	NO	YES	YES
Slurries	NO	NO	NO	YES	YES

SE - standard evaporator

LTVE - long tube vertical evaporator

FFE - falling film evaporator

FCE - forced circulation evaporator

ATFE - agitated thin film evaporator

[a]Strongly dependent upon viscosity

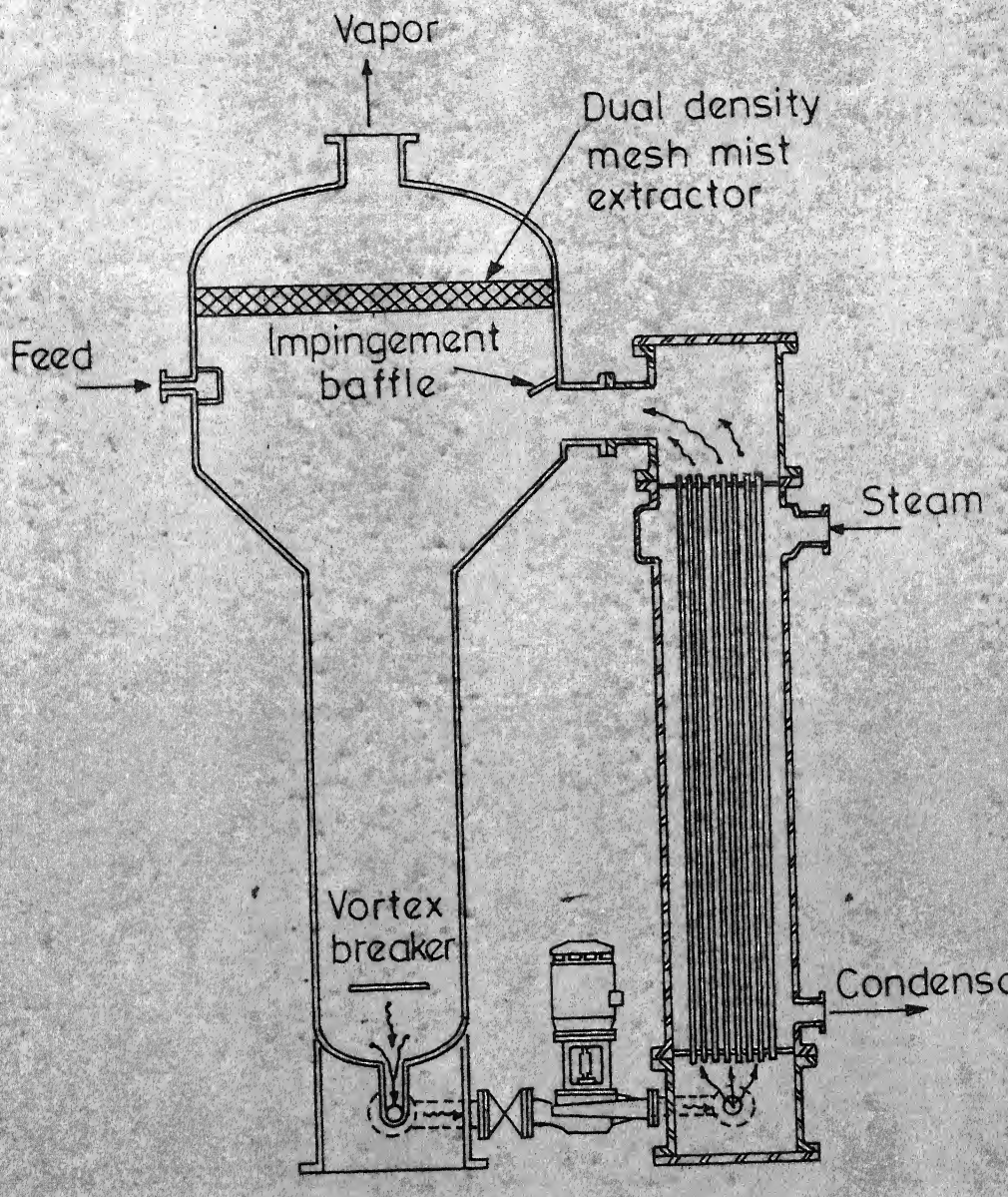

Fig. 1.1 - Forced-circulation vertical evaporator.

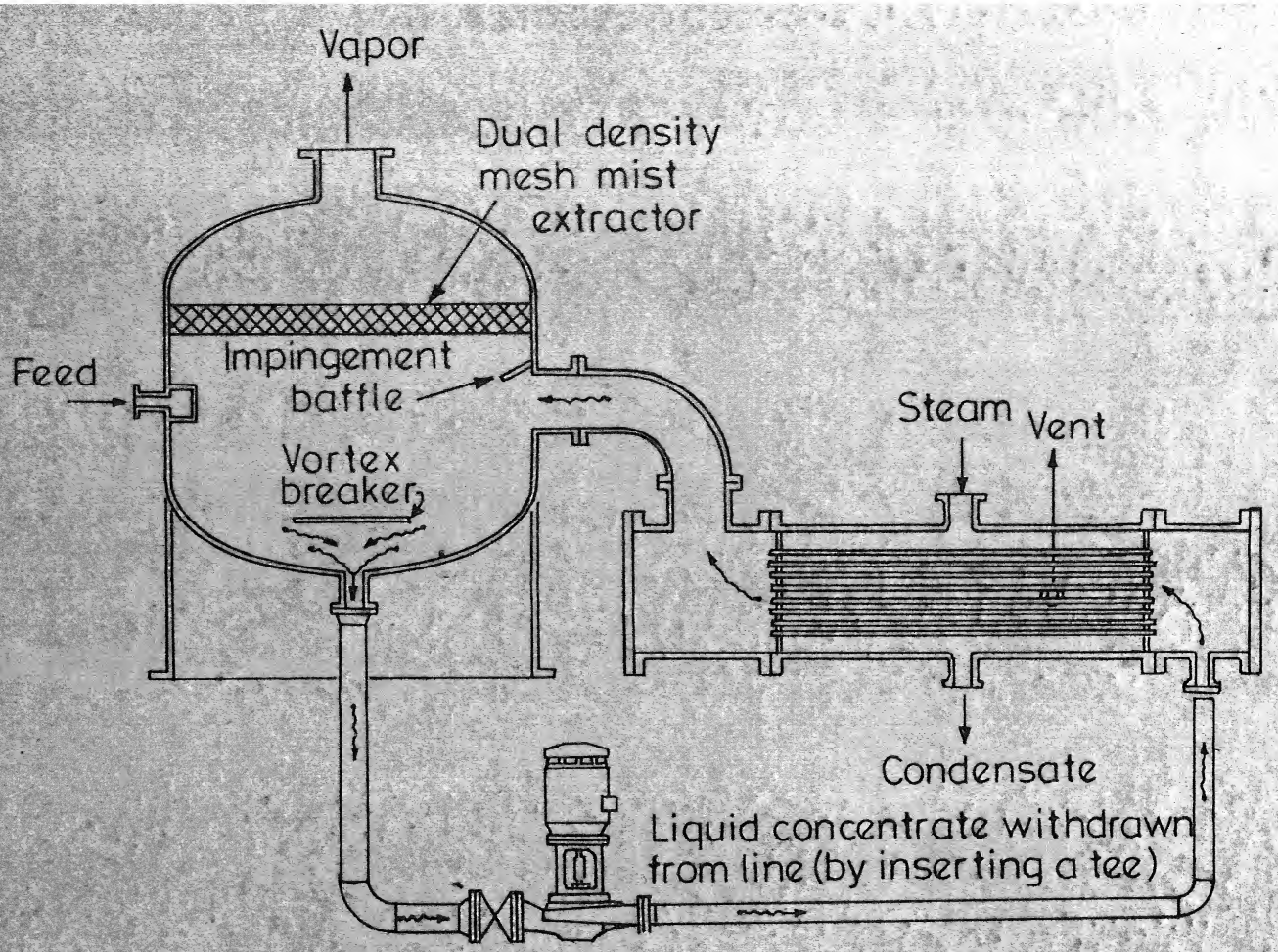

Fig. 1·2 -Forced-circulation horizontal evaporator.

Simulation of an evaporator unit consists in predicting profiles of liquor temperature, concentration, heat flux, overall heat transfer coefficient and evaporation rate. In simulating the performance of an FCE unit process conditions such as flow rate, temperature, concentration, inlet pressure of the feed liquor and vacuum in the seperator, recycle ratio, and steam pressure are generally available. A computer programme is developed in this work to predict the effect of variations in concentration, temperature of feed liquor and recycle ratio on the performance of a FCE unit. Mathematical model required for the simulation is obtained for steady state operation of the evaporator. The model is developed using basic continuity, momentum, and energy balance equations, correlations for pressure drop, hold-up and heat transfer in the non-boiling and boiling zones of the evaporator and the engineering properties of the process liquor. The program gave satisfactory predictions of Badger's [10] boiling heat transfer results with minor modifications to suit experimental conditions. The model was applied to a single tube vertical FCE to study the effect on performance of feed temperature (90-110^{o}C), concentration (35-60 per cent) and rate (5-10 kg/s) for the concentration of black liquor. The model was also used to study the effects of feed concentrations, feed temperature, and recycle ratio, on the performance of a three pass FCE for both horizontal and vertical calendria arrangements

for processing black liquor. The effect of viscosity on performance of FCE was illustrated by bagasse black liquor which has a higher viscosity compared to bamboo black liquor.

CHAPTER 2

HYDRODYNAMICS AND HEAT TRANSFER IN FORCED CIRCULATION EVAPORATOR

Performance of an evaporator depends on temperature drop and overall heat transfer coefficient. Temperature drop is determined by the temperatures of steam and the boiling liquid and boiling point rise. Overall heat transfer coefficient is strongly influenced by equipment geometry, hydrodynamics of fluid flow and various liquid properties like viscosity, thermal conductivity, specific heat, and operation of the unit. During evaporation of viscous solutions over the high concentration range, the resistance of the liquor side film becomes a major factor controlling the overall heat transfer coefficient.

2.1 Forced Circulation (FC) and Natural Circulation (NC) Units:

NC and FC units form two complementary systems of evaporators in many process applications. The former generally constitutes the individual effects of a multiple effect evaporation plant, providing a large increase in liquor concentration. Over the high concentration range the liquors are generally viscous (above 10 cp) and give low heat transfer coefficients in NC units. This limitation is overcome by a FC unit, which circulates the liquor through the tubes at a higher velocity (1-6 m/s) and improves the rate of heat

transfer. For example, in a pulp mill, the evaporation plant consists of a system of multiple effect evaporators having 4-6 effects for the concentration range of 15-55 per cent solids and a FC finisher unit for the range of 55-65 per cent solids. Agarwal [9] has developed a simulation program for a NC long tube vertical evaporator (LTV) typical of the former. This investigation deals primarily with a model for FC evaporator.

Liquor flow pattern in a NC, LTV unit consists of a homogeneous solution in the non-boiling zone and two-phase vapor liquid mixture in the boiling zone. Flow pattern in the boiling zone consists of bubble flow, slug flow and annular flow regions. Agarwal has developed a model based on basic momentum, mass and energy balance equations and correlations describing pressure drop and heat transfer characteristics. Lockhart-Martinelli [16] correlation was used for determining frictional pressure drop for the two-phase mixture in the boiling zone. Coulson-McNelly's [11] and Penman-Tait's [14] correlations were used for the nucleate boiling and annular boiling regions respectively. A maximum in the longitudinal temperature profile was used as the criteria for the transition from non-boiling to boiling zone. A minimum in the profile of pressure gradient [13] was used to determine the transition between nucleate boiling and annular film boiling regions. The model adequately represented the boiling heat transfer

data of Badger [10] and also experimental longitudinal profiles of temperature and heat transfer coefficient of Gudmundson [19]. Fluid flow and heat transfer mechanisms of FCE units depend upon the vertical or horizontal orientation of the calendria and are also influenced by the liquor viscosity, and velocity. These mechanisms are discussed in the next section.

2.2 Hydrodynamics and Heat Transfer:

2.2.1 Flow Pattern in FCE:

Heat transfer in evaporators is intimately related to fluid flow pattern. In the non-boiling zone of FCE fluid is a homogeneous liquid generally in turbulent flow except while handling viscous solutions when the flow can become viscous. In the boiling zone fluid flow pattern is different from that in non-boiling zone. In the boiling zone simultaneous flow of vapour and liquid phases occurs, and the inherent pressure change along the tube continuously changes the phase distribution to give varying longitudinal flow patterns, with corresponding changes in heat transfer mechanisms. A complete hydrodynamic description of the two-phase flow pattern requires a knowledge of the variation of void fraction and distribution of velocity and shear forces in the vapor and liquid phases of the system. Flow patterns in a two-phase vapor-liquid system have been classified according to visual

observation [15,1] and also empirically by Lockhart and Martinell [16] by a combination of laminar or turbulent flow conditions, prevailing for the superficial flow of either phase in the conduit. The spectrum of visually observed flow patterns for two-phase vapor liquid flow is described below.

Bubble Flow: Bubble flow pattern occurs at low void fraction. The liquid phase is continuous and vapor phase distributed in the form of bubbles forming the discontinuous phase in this regime, followed by nucleate boiling heat transfer mechanism.

Slug Flow: In slug flow large slugs of vapor appear in the flow as a result of agglomeration of vapor bubbles. The slugs of vapor accelerate faster than compared to liquid flow and create slip between phases. Slug of liquid and vapor alternate each other and gives rise to instability. This flow pattern would occur at moderate void fractions and relatively low flow velocities. Heat transfer occurs both by nucleate boiling and forced convective mechanisms.

Annular Flow: Increase in vapor velocity results in a central core of vapor flow and an annular climbing film of liquor and heat transfer across the liquid occurs by forced convection.

Mist Flow: With an increase in temperature gradient dry patches begin to appear on the tube surface and liquor droplets are carried as mist by high velocity vapor.

In the boiling zone heat transfer mechanisms are not very distinct, and there is considerable overlap between various mechanisms in the boiling zone. Heat transfer occurs both by nucleate boiling mechanism and forced convection. The convective heat transfer in the boiling zone does not prevent the wall temperature from rising above saturation temperature [21]. As vaporization increases additional nucleation sites are activated and the number of nucleation sites increase and fully developed nucleate boiling occurs. In FC evaporators with vertical calendria the flow pattern is limited to bubble flow as vapor bubbles have little chance to coalesce to form slugs. Coexistence of nucleate boiling and forced convection heat transfer in forced convection vaporization has been experimentally verified [28]. Flow pattern in FCE with horizontal calendria consists of turbulent flow in non-boiling zone, and bubble flow in boiling zone with forced convection and nucleate boiling as the dominant heat transfer mechanisms in the boiling zone.

Lockhart-Martinelli classified the two-phase flow patterns in boiling zone empirically by a combination of laminar or turbulent flow conditions prevailing for the superficial flow of either phase in the conduit. Consequently these flow mechanisms result in laminar-laminar, laminar-turbulent, turbulent-laminar and turbulent-turbulent conditions.

Lockhart-Martinelli parameter is used in heat transfer correlations in Section 2.2.3 for the boiling section.

2.2.2 Pressure Drop Correlations:

Pressure varies along the length of the evaporator tube as the liquid is heated to the boiling temperature in the non-boiling zone leading to two-phase flow of vapor and liquid mixture along the boiling zone. Pressure drop correlations for single phase liquid, would apply to non-boiling section. Pressure drop characteristics of the boiling zone would be based on the hydrodynamics of flow of two-phase mixture. Various factors contributing to pressure drop in the evaporator tube and correlations available for pressure drop are discussed in this section.

2.2.2.1 Pressure Drop for Non-Boiling Zone:

In the non-boiling zone, frictional pressure drop over a differential section of the tube can be determined using equation (2.1).

$$\Delta P_f = \frac{4\,f}{D_i} \cdot \frac{u^2 \rho \Delta z}{2\,g_c} \qquad (2.1)$$

The effect of roughness characteristics of the tube on the value of friction factor can be determined from equations (2.2) and (2.3) for laminar and turbulent flow respectively.

$$f = 16/N_{Re} \qquad (2.2)$$

$$1/f^{1/2} = -2 \log [(\varepsilon/3.7D) + (2.51/N_{Re} \cdot f^{1/2}] \quad (2.3)$$

The above equations are modified to account for the effect of viscosity during non-isothermal flow of the liquid to give equations (2.4) and (2.5) for laminar and turbulent regions respectively.

Divide f by $(\mu_a/\mu_w)^{0.38}$ (2.4)

Divide f by $(\mu_a/\mu_w)^{0.17}$ (2.5)

2.2.22 Pressure drop for Boiling Zone:

Pressure drop will consist of three components - frictional drop, drop due to momentum change, and elevation pressure drop arising from the effect of gravitational field. Equation (2.6) gives the various components of the total pressure drop.

$$\left(\frac{dP}{dZ}\right)_{Total} = \left(\frac{dP}{dz}\right)_f + \left(\frac{dP}{dZ}\right)_m + \left(\frac{dP}{dZ}\right)_e \quad (2.6)$$

Several correlations [15,1-5] are available in literature for estimating the two-phase flow pressure drop, for specific conditions of system geometry, operating conditions and phase properties. In general the two models are available for the analysis of two phase flow: homogeneous model and slip model.

The basic assumptions[16,21]of a homogeneous model are:

1. Equal linear velocity of vapor and liquid phase
2. Thermodynamic equilibrium between phases.
3. A single phase fraction factor applicable to two-phase flow [21].

Homogeneous model considers the two-phase as a single phase possessing certain average properties of each phase. The difficulty with such a model lies in the lack of a suitable method for calculating the pressure gradient due to acceleration.

The alternative slip flow model distinguishes between the vapor and liquid phases which are assumed to flow at different velocities but each at uniform velocity [20]. This model differs from the homogeneous model in that there is slip between liquid and vapor. Momentum and energy balance equations are applied separately for each phase in deriving the model [Chapter 3].

Lockhart-Martinelli [16] developed a procedure for calculating the frictional pressure gradient of an isothermal two-phase flow based on correlation of the data obtained from horizomtal flow of air and various liquids (air-water, hydrocarbon-air) at atmospheric pressure. The expressions of two-phase frictional pressure drop were developed in terms of the contributions of the single phase pressure drop values. The results obtained by Lockhart-Martinelli for isothermal gas-liquid two-phase flow were modified by Martinelli-Nelson[22]

to apply in forced circulation boiling in vertical tubes. Another modification suggested by Levy [25] is the momentum exchange model based on the assumption that the momentum exchange between vapor and liquid phases tend to maintain the frictional and heat losses equal for the two phases. Levy's correlation shows limited agreement for the range of variables considered by Muscettola [26]. This is attributed to the fact that this correlation does not take into account the dependence on mass flow rate, and diverges as the quality approaches one [26]. The various correlations developed for predicting two-phase flow pressure drop are based on data for gas-liquid flow and no generalized correlation is available for predicting pressure drop in two-phase vapor-liquid flow [15]. Dukler et al. [15] have systematically compared existing correlations [21] and found that Martinelli-Nelson correlation predicts frictional pressure drop within ± 30 per cent of measured values [22]. Martinelli-Nelson correlation was also found to be independent of mass flow rates.

2.2.3 Heat Transfer Correlations:

2.2.31 Non-Boiling Zone:

In the non-boiling zone heat transfer to the liquid inside the tube occurs by forced convection. The vast amount of experimental data available in literature, have been satisfactorily correlated by Dittus-Boelter [17] equation (2.7),

valid for $N_{Re} > 10,000$, and $L/D > 60$

$$Nu = 0.0278\ Re^{0.8}\ Pr^{0.4}\left(\frac{\mu_m}{\mu_w}\right)^{0.14} \qquad (2.7)$$

With increase in liquor viscosity, the flow pattern inside the tube can be either in transition on laminar region. For fluids of high viscosity, Coulburn [17, 29] proposed equation (2.8)

$$S_t \cdot Pr^{2/3} = 0.023\ Re^{-0.2} \qquad (2.8)$$

where $S_t = \frac{h}{\rho u C}$ = Stanton Number

The equation (2.8) is recommended for heat transfer to fluids with temperature dependent properties and is applicable for $0.7 < Pr < 160$, $N_{Re} < 10,000$, and $L/D > 60$. In equation (2.8) St is to be evaluated at the average fluid temperature, while N_{Re}, Pr are determined using arithmatic mean of the wall and fluid temperatures. For a large viscosity of the process liquor the flow inside tube can become laminar. In streams flowing in viscous motion natural convection currents can have profound effect on the heat transfer. Studies of natural convection have shown that Grashoff number satisfactorily correlated a heat transfer data for viscous flow. Grashoff Number introduces the added influence of natural convection currents contributing to heat transfer in forced convection in the viscous region. Eubank and Proctor [17] critically surveyed the available data for viscous flow and

arrived at the following empirical equation (2.9).

$$(Nu)\left(\frac{\mu_w}{\mu}\right)^{0.14} = 1.75 \left[(Gz) + 0.04 \left[(D/L)(Gr)(N_{Re})\right]^{0.75}\right]^{1/3} \quad (2.9)$$

Equation (2.9) can be used to determine the heat transfer coefficient for laminar flow region.

2.2.32 Boiling Zone:

Prediction of heat transfer coefficient for boiling of liquids in forced convection is very much of interest in practice, due to wide spread use of boiling reactors in nuclear power generation. But no fundamental theory is yet available to predict the boiling heat transfer coefficient for forced convective boiling. In order to achieve a meaningful correlation of heat transfer coefficient for two-phase vapor liquid flow, as encountered in boiling, it is necessary to measure local heat fluxes and temperature differences. Dengler and Addoms[12], Guerrieri and Talty [31], Bennet [23] and Schrock and Grossman [32] have measured such coefficient for the boiling of liquid in vertical tubes and annuli.

In the forced convective region, Dengler and Addoms[12], and also Guerrieri and Talty correlate their results according to equation (2.10) by analogy to analysis of Lockhart and Martinelli.

$$\frac{h_{TP}}{h_{LP}} = A\left[\frac{1}{X_{tt}}\right]^{n} \qquad (2.10)$$

where h_{LP} and h_{TP} denote heat transfer coefficient for superficial liquid and two phase vapor liquid flow respectively.

X_{tt} - Lockhart-Martinelli parameter [Appendix A]

$$h_{LP} = 0.023 \frac{k_L}{D_i}\left[\frac{D_i\, G(1-x)}{\mu_L}\right]^{0.8}\left[\frac{C_P\, \mu_L}{k_L}\right]^{0.4} \qquad (2.11)$$

Values of the coefficients in equation (2.10) reported by different authors, are as follows:

Dengler and Addoms:	A = 3.5,	n = 0.5
Wright :	A = 2.72	n = 0.58
Schrock and Grossman:	A = 2.5	n = 0.75
Collier and Pulling:	A = 2.7	n = 0.7

Departure of experimental results from these correlations in all cases was attributed to appreciable contribution by nucleate boiling towards heat transfer. These correlations do not take into consideration influence of nucleate boiling. Schrock and Grossman have proposed equation (2.12) which also includes the effect of nucleate boiling.

$$\frac{h_{TP}}{h_{LP}} = B\left[\frac{Q}{G \cdot \lambda_v}\right] + A\left[\left(\frac{1}{X_{tt}}\right)^{n}\right] \qquad (2.12)$$

Q - heat flux

G - total mass flux

λ_v - heat of vaporization

$\frac{Q}{G \cdot \lambda_v} = B_o$, bubble Number

The following values of constants B, A, n have been reported by Schork-Grossman [32] and Wright [33].

Schrock-Grossman: $B = 7.39 \times 10^3$, $A = 1.5 \times 10^{-4}$, $n = 0.66$

Wright : $B = 6.70 \times 10^3$, $A = 3.5 \times 10^{-4}$, $n = 0.66$.

Schrock and Grossman studied the following range of conditions.

System: Water-steam in vertical stainless steel tube

Tubes: 0.118 in I.D. x 15,30, 40 in long

0.237 in I.D. x 15 and 30 in long

0.432 in I.D. x 30 in long

Pressure: 42-505 psia

Quality: 5-57 per cent

Schrock and Grossman obtained $\pm$ 30 per cent fit of the experimental data with the mentioned constants.

It is expected that the contributions of the nucleate boiling heat transfer and forced convective heat transfer vary with flow conditions. These variations have been investigated by Chen [34]. Chen obtained empirically the values of two dimensionless functions S and F, that allow for the variations in the nucleate boiling and forced convective components respectively.

$$h_{TP} = S \cdot h_{nucleate} + F \cdot h_{forced\ convection} \qquad (2.13)$$

This correlation agrees very well with wide range of experimental data [23,12]. Chen uses Forster-Zuber's [35] nucleate boiling heat transfer correlation and the Dittus-Boelter forced convective heat transfer correlation. At the present time no generalized correlation is available for prediction of nucleate boiling heat transfer coefficient.

2.3 Correlations Recommended for FCE:

2.3.1 Pressure Drop Correlations:

Equation (2.1) can be used to predict pressure drop over non-boiling zone reliably. The equation (2.1) is independent of any system, as long as the liquid is Newtonian. Pressure drop correlations for boiling zone in FCE are not many. Martinelli-Nelson correlation has been tested for forced circulation boiling of water, and this predicts experimental data within $\pm$ 30 per cent. This correlation can be recommended for boiling zone in FCE equation (A.7).

2.3.2 Heat Transfer Correlations:

Equations (2.7) to (2.9) can predict accurately heat transfer coefficient in non-boiling zone of FCE. For predicting film coefficient in boiling zone in FCE, Schrock-Grossman correlation is recommended. This correlation has been developed for forced circulation vaporization of water in stainless steel tubes. This correlation takes into account both the mechanisms of heat transfer in the boiling zone.

The range of heat flux and pressure considered by Schrock-Grossman agrees with FCE conditions. This correlation is expected to predict film coefficient for boiling zone well.

2.3.3 Recommendations for Kraft Black Liquor System:

Present work considers kraft black liquor as the process fluid in the FCE unit. Black liquor was selected since the correlations for various engineering properties are readily available from previous work [36,37]. The various correlations discussed earlier have been developed for systems different from black liquor. Comments on the applicability of these correlations for the black liquor system are given in this section.

Pressure drop for non-boiling zone can be reliably predicted from equation (2.1). This equation is dependent only on density, friction factor Reynold's number. Film coefficient for black liquor in non-boiling zone can be predicted from equations (2.7) to (2.9). Harvin [17] has worked extensively with black liquor system and verified the validity of the equations (2.7) to (2.9) for predicting film coefficient in horizontal tubes for laminar transition and turbulent flow conditions for the concentration range of 30 to 60 per cent solids.

Martinelli-Nelson correlation, based on experimental data for forced convective vaporization of water and Lockhart-

Martinelli parameter for frictional pressure drop, gave satisfactorily prediction for the pressure range of 120 to 20000 kN/m^2 [22] and quality 4 to 95 per cent. Because of the applicability of Martinelli-Nelson over a wide range of pressure and quality it is recommended for black liquor system even tho gh the effect of viscosity is not included in Martinelli-Nelson correlation. It is assumed that Martinelli-Nelson equation will give a satisfactory estimate of pressure drop, over a moderate range of values.

Prediction of film coefficient in boiling zone also raises the question of applicability of Schrock-Grossman correlation for black liquor system. Even though the correlation considers both nucleate and forced convective mechanisms, for water, the effect of viscosity is not well defined. A complex system of like black liquor is not convenient in fundamental studies of 2-phase flow heat transfer/fluid flow mechanisms. In the present work the viscosity range is 4 to 30 cp and the liquid is Newtonian. Schrock-Grossman correlation will overestimate the heat transfer coefficient by probably 30 per cent. This limitation must be borne in mind while interpreting the results obtained by the simulation model of this study for the black liquor system.

CHAPTER 3

MATHEMATICAL MODEL OF FORCED CIRCULATION EVAPORATOR

Simulation requires simultaneous mathematical description of the hydrodynamic and heat transfer phenomena occurring along the length of the evaporator tube. The present study deals mainly with steady state simulation. Mathematical model for the evaporator is developed from basic energy, continuity and momentum balance equations and correlations available in current literature for heat transfer in non-boiling and boiling zones of the evaporator tube. Simulation of an evaporator unit consists in predicting longitudinal profiles of liquor temperature, concentration, heat flux, overall heat transfer coefficients and evaporation rate. To obtain overall performance a differential approach is adopted by considering the tube length to consist of a series of differential segments (dz). Momentum, energy balance, continuity equations together with various correlations are applied for a differential length (dz) to obtain mathematical expressions which predict changes in liquor conditions over the differential length (dz) by an iterative procedure. The desired longitudinal profiles are then obtained by a sequential traverse of the non-boiling and boiling zones of the entire tube length. The model is developed

for an evaporator with vertical calendria and the modifications necessary for a horizontal calendria are discussed in Section 3.4

3.1 FCE with Vertical Calendria:

3.1.1 Non-Boiling Zone:

Energy, momentum and continuity equations are applied over a differential length (dz) for the one dimensional analysis of the single phase flow in the non-boiling section (Fig. 3.1a). The following assumptions are used in the analysis.

1. Radial variations in parameters like pressure, density, temperature, velocity and other transport properties are considered to be small.
2. Steam is at saturation temperature.
3. Heat losses are negligible.

3.1.2 Momentum Balance:

Equation (3.1) gives the momentum balance for the differential section.

$$\sum F = \text{Rate of change of momentum of fluid} \qquad (3.1)$$

$$\text{Momentum input} = \frac{\rho_F u_F A}{g_c} u_F$$

$$\text{Momentum output} = \frac{(\rho_F + d\rho_F)(u_F + du_F)A}{g_c} (u_F + du_F)$$

$$\text{Change in momentum} = \frac{A}{g_c}\left[(\rho_F + d\rho_F)(u_F + du_F)^2 - \rho_F u_F^2\right] \qquad (3.2)$$

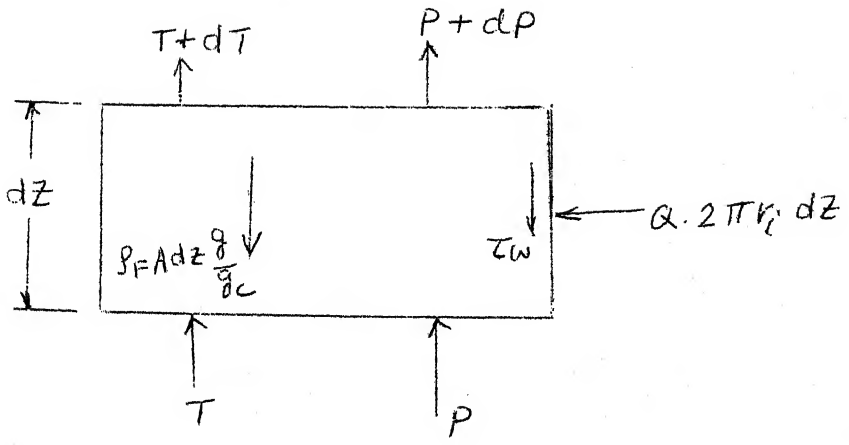

FIGURE 3.1a: DIFFERENTIAL SEGMENT IN NON-BOILING ZONE

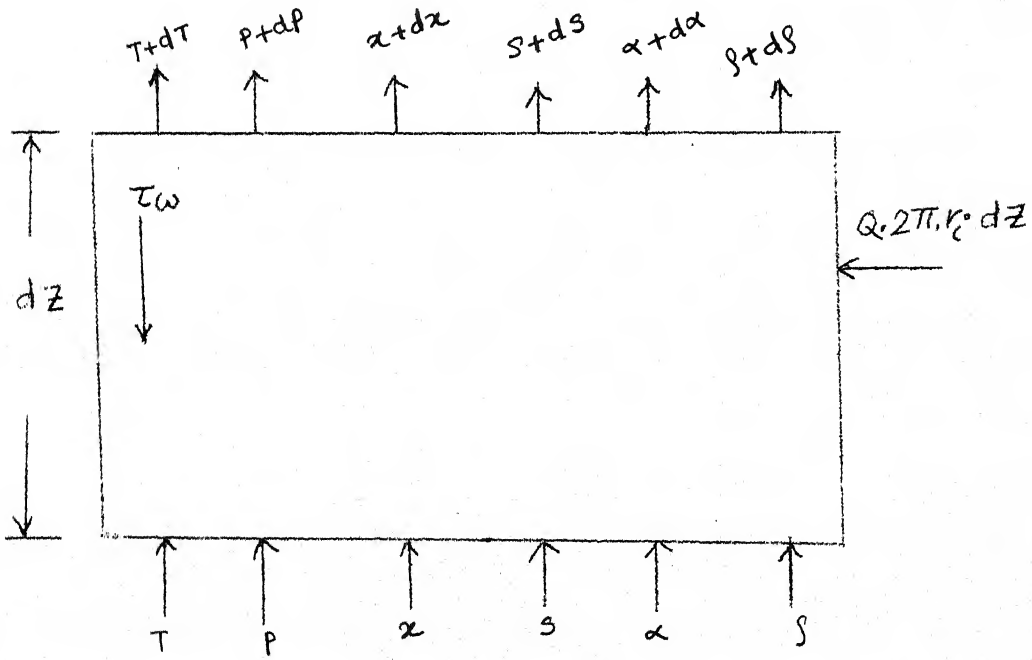

FIGURE 3.1b: DIFFERENTIAL SEGMENT IN BOILING ZONE

Equation (3.3) represents material balance

$$A \rho_F u_F = \text{Constant}$$

$$d(A \rho_F u_F) = 0$$

$$\rho_F \, du_F = - u_F \, d\rho_F \qquad (3.3)$$

Combining equations (3.2) and (3.3) gives change in momentum:

$$\frac{A}{g_c} [u_F \rho_F \, du_F] \qquad (3.4)$$

Equation (3.5) gives net forces acting upward on the fluid element and include contributions from pressure, hydrostatic head and shear forces.

$$A.P - A\cdot(P + dP) - \bar{\rho}_F \cdot A \cdot dz \cdot \frac{g}{g_c} - \tau_w \cdot \pi \cdot D_i \cdot dz \qquad (3.5)$$

Equation (3.6) relates frictional pressure drop and shear stress at the wall.

$$\tau_w \cdot \pi \cdot D_i \cdot dz = dP_f \cdot \pi \cdot D_i^2/4$$

$$\tau_w = \frac{dP_f}{dz} \cdot \frac{D_i}{4} \qquad (3.6)$$

Net upward force on the fluid element is obtained by combining equations(3.5) and (3.6) to give (3.7)

$$-A\cdot dP - \bar{\rho}_F \cdot A \cdot dz \cdot \frac{g}{g_c} - \frac{dP_f}{dz} \cdot A \cdot dz \qquad (3.7)$$

Substitution of the above expressions for the various terms of equation (3.1) results in equation (3.8) for the prediction

of pressure gradient along the length for the non-boiling zone.

$$\frac{dP}{dz} = - \bar{\rho}_F \cdot \frac{g}{g_c} - \left(\frac{dP_f}{dz}\right) - \frac{u_F \bar{\rho}_F \, du_F}{g_c \, dz} \qquad (3.8)$$

3.1.3 Total Energy Balance:

The general form of total energy balance equation is as follows:

$$d(\text{Enthalpy}) + d(\text{Kinetic Energy}) + d(\text{Potential Energy}) = dQ \qquad (3.9)$$

The calculation of each term in equation (3.9) for the differential section is shown below.

d(Enthalpy) = Enthalpy of liquid leaving - Enthalpy of liquid entering

$$= \bar{W}_T[(C_F + dC_F)(T+dT - T_o) - C_F(T-T_o)]$$

$$= \bar{W}_T[C_F \, dT + dC_F \, (T-T_o)]$$

$$d(\text{Kinetic Energy}) = \frac{1}{2} \bar{W}_T \left[\frac{(u_F + du_F)^2}{g_c J} - \frac{u_F^2}{g_c J}\right]$$

$$= \bar{W}_T\left[\frac{u_F \, du_F}{g_c J}\right]$$

$$d(\text{Potential Energy}) = \bar{W}_T \cdot \frac{g}{g_c J} \cdot dz$$

Replacing individual terms in equation (3.9) and assuming a constant value for specific heat (C_F) gives equation (3.10)

for predicting the change in temperature of liquor (dT).

$$W_T\left[C_F\, dT + \frac{u_F \cdot du_F}{g_c J} + \frac{g}{g_c J}\, dz\right] = Q_i\, \pi\, D_i\, dz$$

$$dT = \frac{1}{C_F}\left[\frac{Q_i\, \pi\, D_i\, dz}{W_T} - \frac{u_F\, du_F}{g_c J} - \frac{g}{g_c J}\, dz\right] \qquad (3.10)$$

3.1.4 Boiling Zone:

The following simplifying assumptions are made for developing necessary equations applicable to the boiling zone.

1. Flow is one dimensional
2. Negligible radial variations of velocity, pressure, temperature and quality.
3. Equilibrium exists between vapor and liquid in the boiling zone.
4. Density, viscosity, and other transport properties are taken as weighted average of the mixture.

3.1.5 Momentum Balance:

Application of momentum balance equation (3.1) to a differential section dz in the boiling zone will give (3.11) for the total pressure gradient (Figure 3.1b)

$$\left(\frac{dP}{dz}\right)_t = -\left(\frac{dP}{dz}\right)_f - \left(\frac{dP}{dz}\right)_a - \left(\frac{dP}{dz}\right)_e \qquad (3.11)$$

$\left(\frac{dP}{dz}\right)_t$ = Total pressure gradient

$\left(\frac{dP}{dz}\right)_f$ = Frictional pressure gradient obtained by Martinelli-Nelson correlation [22].

$\left(\frac{dP}{dz}\right)_e$ = Pressure gradient due to elevation change

$\left(\frac{dP}{dz}\right)_a$ = Accelerative pressure gradient (discussed in Appendix A)

$$= \frac{G_T^2}{g_c} \frac{d}{dz}\left[\frac{(1-x)^2}{\rho_F(1-\alpha)} + \frac{x^2}{\rho_v \alpha}\right] \qquad (3.12)$$

Density and viscosity of the two phase mixture are taken as the weighted average of the values of the separate phases using quality (x) as represented by equation (3.13)

$$1/\bar{\rho} = \frac{1-x}{\rho_F} + \frac{x}{\rho_v} \qquad (3.13a)$$

$$1/\bar{\mu} = \frac{1-x}{\mu_F} + \frac{x}{\mu_v} \qquad (3.13b)$$

3.1.6 Total Energy Balance:

Enthalpy of mixture leaving dz:

$$W_T(1-x-dx)\, C_F(T+dT-T_o) + W_T(x+dx)\, C_v(T+dT-T_o) + W_T(x+dx)\lambda_v$$

Enthalpy of mixture entering dz:

$$W_T(1-x).(T-T_o) + W_T\, C_v\, x\, (T-T_o) + W_T x\, \lambda_v$$

$$d(\text{Enthalpy}) = W_T \cdot C_F(1-x)\, dT - W_T C_F \cdot (T-T_o) \cdot dx + W_T \cdot C_v x \cdot dT + W_T \cdot C_v (T-T_o) dx + W_T \cdot dx\, \lambda_v$$

$$d(\text{Kinetic Energy}) = \frac{G_T^2}{2g_c J} \; d\left[\frac{x^3}{\rho_v^2 \alpha^2} + \frac{(1-x)^3}{\rho_F^2 (1-\alpha)^2} \right]$$

Substituting the individual terms in the total energy equation gives equation (3.14)

$$dT = \frac{1}{C_F(1-x) + C_v x} \left[\frac{Q_i \; \pi \; D_i \; dz}{W_T} + C_F(T-T_o)dx - C_v \; (T-T_o)dx \right.$$

$$\left. -dx\lambda_v - \frac{G_T^2}{2g_c} \; d \left(\frac{x^3}{\rho_v^2 \alpha^2} + \frac{(1-x)^3}{\rho_F^2 (1-\alpha)^2} \right) - \frac{g}{g_c J} \; dz \right] \qquad (3.14)$$

Equation (3.14) can be rearranged to give equation (3.15) for predicting the change in quality 'dx', by choosing T as the reference temperature.

$$dx = \frac{1}{\lambda_v} \left[\frac{Q_i \; \pi \; D_i \; dz}{W_T} - \frac{G_T^2}{2 \; g_c J} \; d\left[\frac{x^3}{\rho_v^2 \; \alpha^2} + \frac{(1-x)^3}{\rho_F^2 (1-\alpha)^2} \right] \right.$$

$$\left. - \frac{g}{g_c J} \; dz - dT \left[C_v x + C_F(1-x) \right] \right] \qquad (3.15)$$

3.2 Mass Balances:

3.2.1 Solute Balance in Boiling Zone:

Solute balance over the differential section gives equation (3.16) for predicting changes in liquor concentration.

$$W_T \; (1-x)S \; = W_T(1-x-dx) \; (S + dS)$$

$$dS \; = \frac{S \cdot dx}{1-(x+dx)} \qquad (3.16)$$

3.2.2 General Mass Balance for Evaporator with Recycle:

Figure 3.2 gives different variables associated with the streams for an evaporator arranged for recycle of a portion of the product to accomplish the necessary rise in liquor concentration.

Total material balance:

$$W_v = W_1 - W_2 \tag{3.17}$$

Total Solid balance:

$$W_1 S_1 = W_2 S_2 \tag{3.18}$$

Recycle ratio:

$$R = \frac{W_R}{W_2} \tag{3.19}$$

Total feed to evaporator:

$$W_T = W_1 + W_R = W_1 + RW_2$$

$$= W_1 + \frac{W_1 S_1}{S_2} R$$

$$= W_1 \left(1 + \frac{S_1}{S_2} \cdot R\right) \tag{3.20}$$

Inlet liquor concentration to the evaporator tube,

$$S_i = \frac{W_1 S_1 + W_R S_2}{W_1 + W_R} = \frac{W_1 S_1 (1+R)}{W_T} \tag{3.21}$$

3.3 Material and Energy Balance for Flash Separator:

Liquid issuing from tubes is flashed in vapor space and achieves an additional increase in liquor concentration. Vapor space is invariably maintained under vacuum,

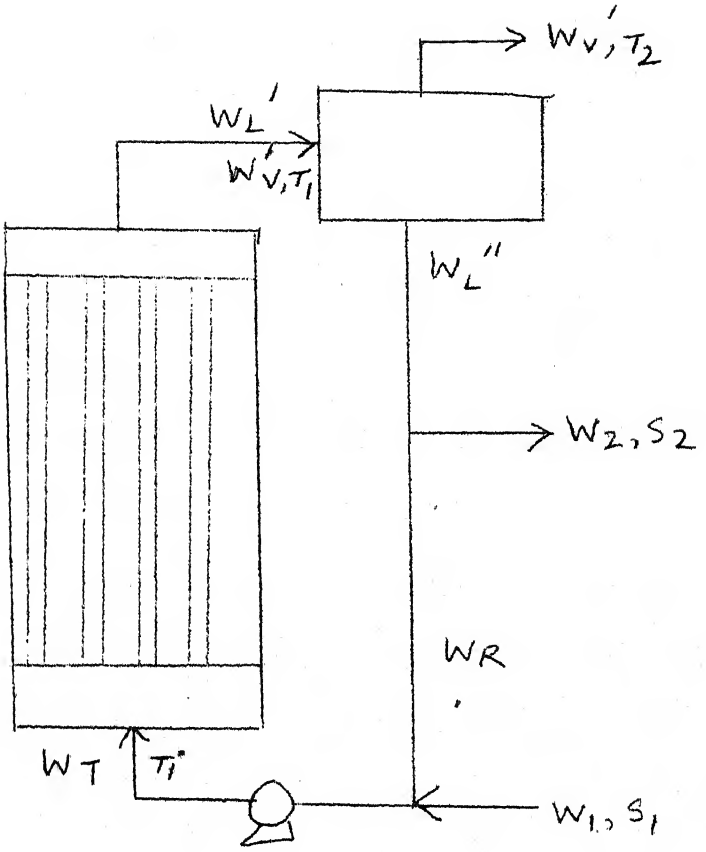

FIGURE 3.2: SCHEMATIC DIAGRAM OF A FORCED CIRCULATION EVAPORATOR WITH RECYCLE SHOWING VARIOUS STREAMS

and connected to an intermediate effect of a multiple effect evaporation plant. A large chamber is used for flashing to reduce the velocity of vapor stream and to reduce entrainment of liquor droplets.

Temperature of liquor leaving flash tank (T_2) is taken as reference temperature for energy balance equations of the separator.

Equations (3.22) and (3.23) represent inlet (H_i) and exit enthalpies of the vapour-liquid mixture.

$$H_i = W'_L C'_L(T_1-T_2) + W'_v C'_v (T_1-T_2) + W'_v \lambda'_v \quad (3.22)$$

$$H_o = W_v \lambda''_v + W_v C_v (T_2-T_2) + W''_L C''_L (T_2-T_2) \quad (6.23)$$

$$W_v = W'_v + W''_v$$

Enthalpy balance gives equation (3.24)

$$W'_L C'_L (T_1-T_2) + W'_L C'_v (T_1-T_2) + W'_v \lambda'_v = W_v \lambda''_v \quad (3.24)$$

Total material balance around flash separation

$$W_v = W'_v + W'_L - W''_L$$

Substituting for W_v in enthalpy balance gives equation (3.25) for the rate of flash liquor

$$W''_L = \frac{W'_v[\lambda''_v - \lambda'_v - C'_v(T_1-T_2)] + W'_L[\lambda''_v - C'_L(T_1-T_2)]}{\lambda''_v} \quad (3.25)$$

Liquor concentration after flashing is calculated from equation (3.18)

3.4 Modifications for Evaporator with Horizontal Calendria:

Evaporations with horizontal calendria, have a horizontal heating element. To predict the necessary profiles, elevation terms are deleted from equations (3.8), (3.10), (3.11) and (3.15). Equations (3.8) and (3.10) for the non boiling zone are arranged to give equations (3.26) and (3.27)

$$\left(\frac{dP}{dz}\right) = -\left(\frac{dP_F}{dz}\right) - \frac{u_F \rho_F du_F}{g_c} \qquad (3.26)$$

$$dT = \frac{1}{C_F}\left[\frac{Q_i \pi D_i dz}{W_T} - \frac{u_F du_F}{g_c J}\right] \qquad (3.27)$$

For the boiling zone, equation (3.15) is modified to equation (3.28) for predicting change in quality (dx).

$$dx = \frac{1}{\lambda_v}\left[\frac{Q_i \pi D_i dz}{W_T} - \frac{G_T^2}{2g_c J} d\left(\frac{x^3}{\rho_v^2 \alpha^2} + \frac{(1-x)^3}{\rho_F^2 (1-\alpha)^2}\right) - dT\left\{C_F(1-x) + C_v x\right\}\right] \qquad (3.28)$$

Simulation computations are carried out in a stepwise manner assuming a series of differential sections of the evaporator tube, and using the criteria of maxima in liquor temperature profile for the transition from non-boiling to boiling zone[10].

3.5 Engineering Properties of Process Liquor:

Computations require correlations for engineering properties process liquors. Necessary engineering data and

correlating are available for kraft black liquor system from earlier work [36,37].

(a) Density (g/cc):

$$\rho_L = 1.0182 + 0.779 \cdot S - (0.000219 + 0.0003 \cdot S(\cdot T \qquad (3.29)$$

(b) Thermal conductivity (kcal/hr.m ^{o}C)

$$k_L = 0.53354269 - 0.3425 \cdot S + (0.0011355 + 0.000209 \cdot S) \cdot T \qquad (3.30)$$

(c) Specific Heat(kcal/kg ^{o}C)

$$C_L = 0.993 - 1.25 \cdot S + (0.0000506 + 0.0104 \cdot S) \cdot T \qquad (3.31)$$

(d) No generalized correlation is available for viscosity of black liquor in the concentration range 35-60 per cent. Table 3.1 gives viscosity data for bamboo kraft black liquor over a range of concentration and temperature values. From the available experimental data a correlation of the form

$$\log\mu = A + \frac{B}{(T + 273)} + \frac{C}{(T+273)^2} \qquad (3.32)$$

has been d eveloped by polynomial regression analysis, for each reported concentration of black liquor. Viscosity for a concentration of black liquor, intermediate between two successive concentrations of Table 3.1 is estimated by linear interpolation.

TABLE 3.1

VISCOSITY BAMBOO KRAFT BLACK LIQUOR

Percent solid	Temperature, °C						
	50	60	70	80	90	100	110
35	10.23	7.71	5.80	4.37	3.29	2,48	1.88
40	21.58	14.64	10.45	7.81	6.06	4.87	4.03
45	40.26	25.66	16.77	11.22	7.66	5.33	3.78
50	68.27	41.52	27.23	14.06	14.11	10.98	8.91
55	173.97	99.00	61.63	41.58	29.98	22.93	18.45

TABLE 3.2

PROPERTIES OF LIQUID WATER

Temperature °C	Viscosity cp	Thermal Conductivity, kcal/h m °C	Density gm/cc
38	0.682	0.539	0.994
49	0.559	0.552	0.989
60	0.470	0.563	0.984
71	0.401	0.572	0.978
82	0.347	0.578	0.971
93	0.305	0.584	0.964
104	0.270	0.587	0.954

(e) Boiling Point Elevation (^{o}C)

$$BPR = (-2.57709 + 30.7781 \cdot S + 1.49186 \cdot S^3)/1.8 \quad (3.33)$$

(f) Vapor Pressure - Temperature Relationship for Water:

Vapor pressure and temperature can be correlated by Antoine equations (3.14) and (3.15)

$$\log P = A - \frac{B}{T-BPR+C} \quad (3.34)$$

$$T = \frac{B}{A-\log P} - C + BPR \quad (3.35)$$

(g) Properties of liquid water as a function of temperature has been generated from Table 3.2 by linear interpolation.

3.6 Void Fraction Correlation:

In the boiling zone correlation for predicting void fraction is available from literature. Anthony etal have obtained correlation by regression analysis of large volume of data [1-9]. The correlation is given by equation (3.36).

$$\alpha = \exp[-0.25522 - 0.10583 \cdot \ln(X) - 0.0289 \cdot (\ln(X))^2 - 0.00884 \cdot (\ln(X))^2] \quad (3.36)$$

α - Fraction of volume occupied by vapor in a mixture of vapor and liquid.

X - Lockhart Martinelli Parameter.

3.7 Computational Scheme:

Simulation computations are carried out in a stepwise manner assuming a series of differential sections of the evaporation tube and using a criteria of maxima in liquor temperature profile for transition from non-boiling to boiling zone.

3.7.1 Computational Algorithm for Non-Boiling Zone:

For a weak black liquor feed below its saturation temperature, flow chart of computation for the non-boiling section is given in Figure 3.3. Flow rate, concentration temperature, pressure, recycle ratio, steam chest temperature, and tube geometry are fixed for starting calculations. A differential length (dz) of tube is considered to determine the heat transfer rates. Temperature differential dT is assumed first. Liquor properties at mean temperature, T+dT/2 is evaluated. The change in pressure in this section is calculated from the frictional pressure drop correlation equations (3.8), (2.1), (2.3), (2.5), (3.26).
The overall heat transfer coefficient for the differential section is calculated from the individual film coefficients for liquid and steam sides and resistances of the wall and scale deposits. Heat flux is computed from heat transfer rate equation ($Q = U.\Delta T$). Equation (3.10), (3. 27) are used to determine differential change in temperature dT and compared with initial assumption. If the calculated value

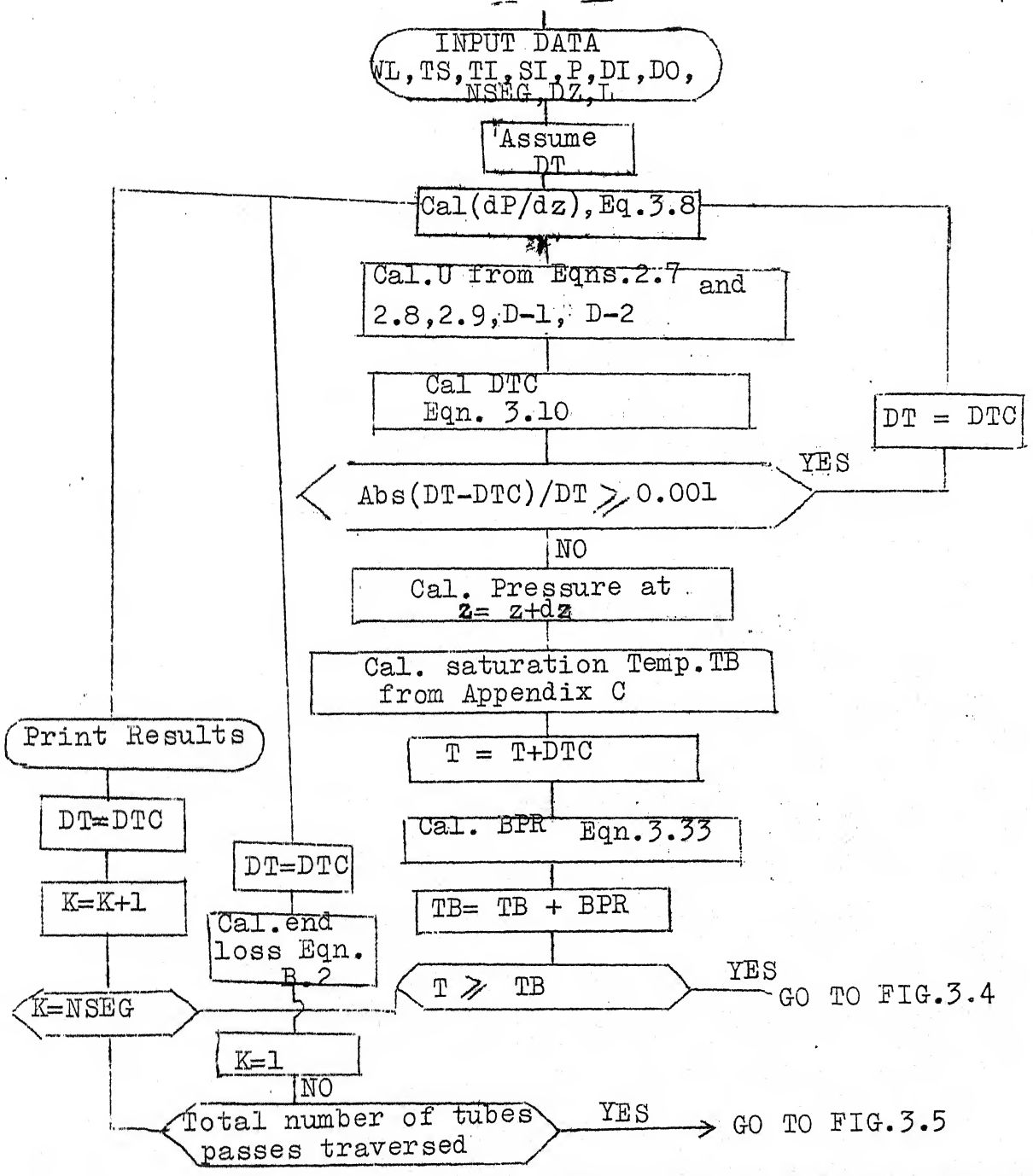

FIGURE 3.3: COMPUTATIONAL ALGORITHM FOR NON-BOILING SECTION

and assumed value differ by more than a preassigned limit, calculation is repeated with new value of dT. Otherwise calculated liquor temperature is compared with saturation temperature, corresponding to pressure at the exit of the differential section. If the liquid temperature happens to be below the saturation temperature, calculation is continued for next section with a new assumed value of dT. This process is repeated until the liquor temperature equals the saturation temperature of liquor. This point corresponds to the end of non-boiling regime, and subsequent calculations are carried out for boiling section.

3.7.2 Computational Algorithm for Boiling Zone:

The whole tube length is divided into a fixed number of segments. Computational algorithm for estimating changes in the process liquor conditions in the boiling section is given in Figure 3.4. A differential section of length (dz = 0.1 m) is considered in the boiling section. Calculations over the differential section give the change in liquor to temperature, pressure, pressure gradient, concentration, quality, void fraction heat flux and overall heat transfer coefficient. Value for the change in dT is assumed for the differential section. Pressure gradient over the differential section is calculated using equations(3.11) to (3.13) and correlation given in Appendix A. Total pressure drop over the differential section is obtained by multiplying pressure

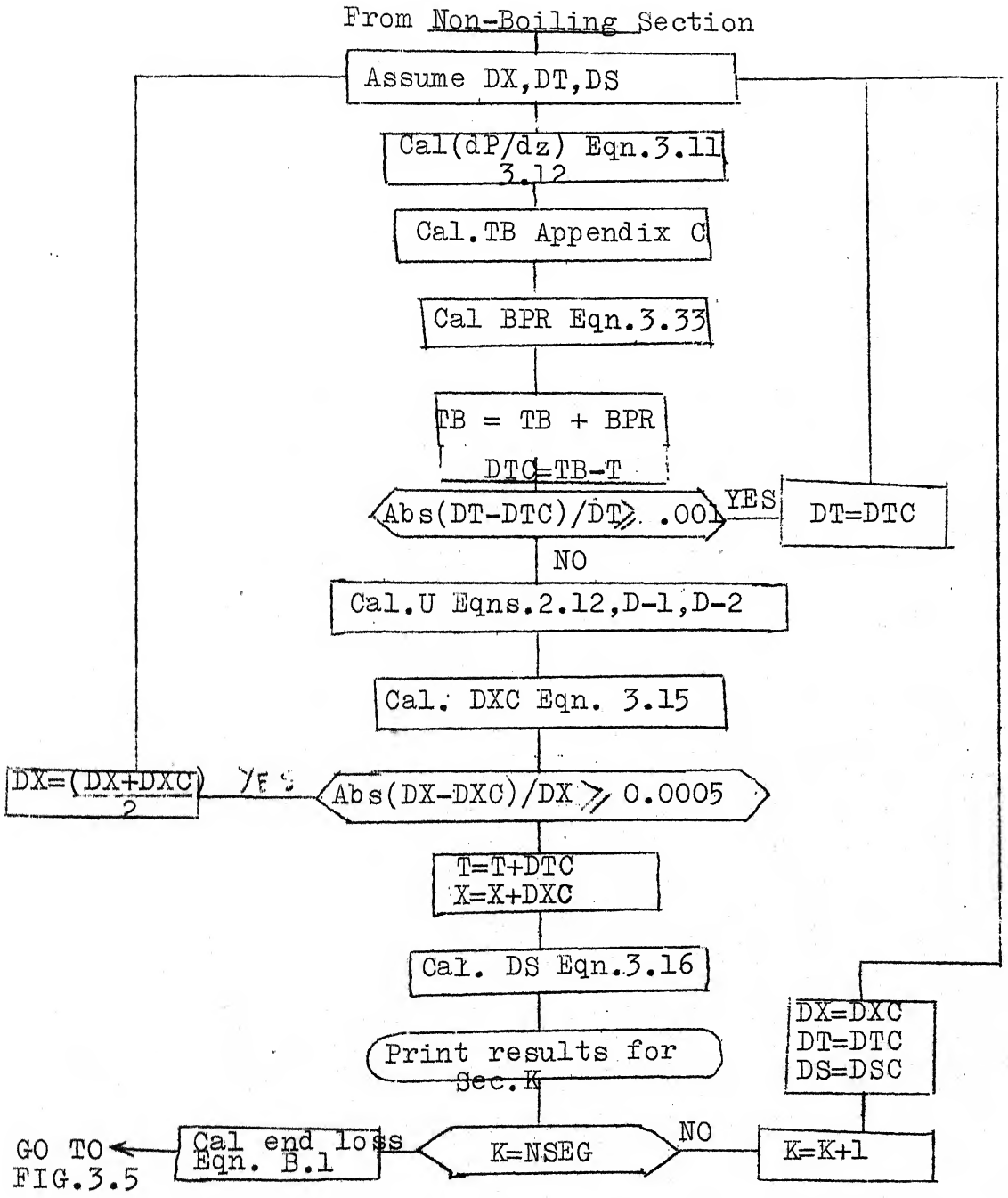

FIGURE 3.4: COMPUTATION ALGORITHM FOR BOILING SECTION

gradient by dz. The temperature at the end of the exit of the differential section is calculated from vapor-liquid equilibrium for water (Appendix - C), corresponding to the pressure at the exit of the differential section. To this temperature boiling point rise is included. Overall heat transfer coefficient is calculated from individual film coefficients, and contributions of the tube wall and dirt resistances. Heat flux Q is calculated from $Q=U \cdot \Delta T$ and equation (3.15)is used to calculate change in quality. It is assumed that vapor and liquid remain in equilibrium, and calculated dT is compared with assumed dT for convergence. When temperature difference dT has been determined, change in quality (dx), and liquor concentrations (dS) are determined from equations.(3.15),(3.16)A counter 'K' keeps track of number of segments calculated and calculation is stopped when 'K' reaches 'NSEG' total number of segments in a pass. Similarly calculation is repeated for next pass, and continued until calculation for the all passes are completed.

3.7.3 Computational Algorithm for Flash Calculation:

In FCE major portion of evaporation takes place in the vapor separator and the change in liquor concentration is computed according to Figure 3.5 . Initially outlet liquor concentration S_2 is assumed. From equation (3.18) flow rate of concentrated liquor is calculated. For a given recycle

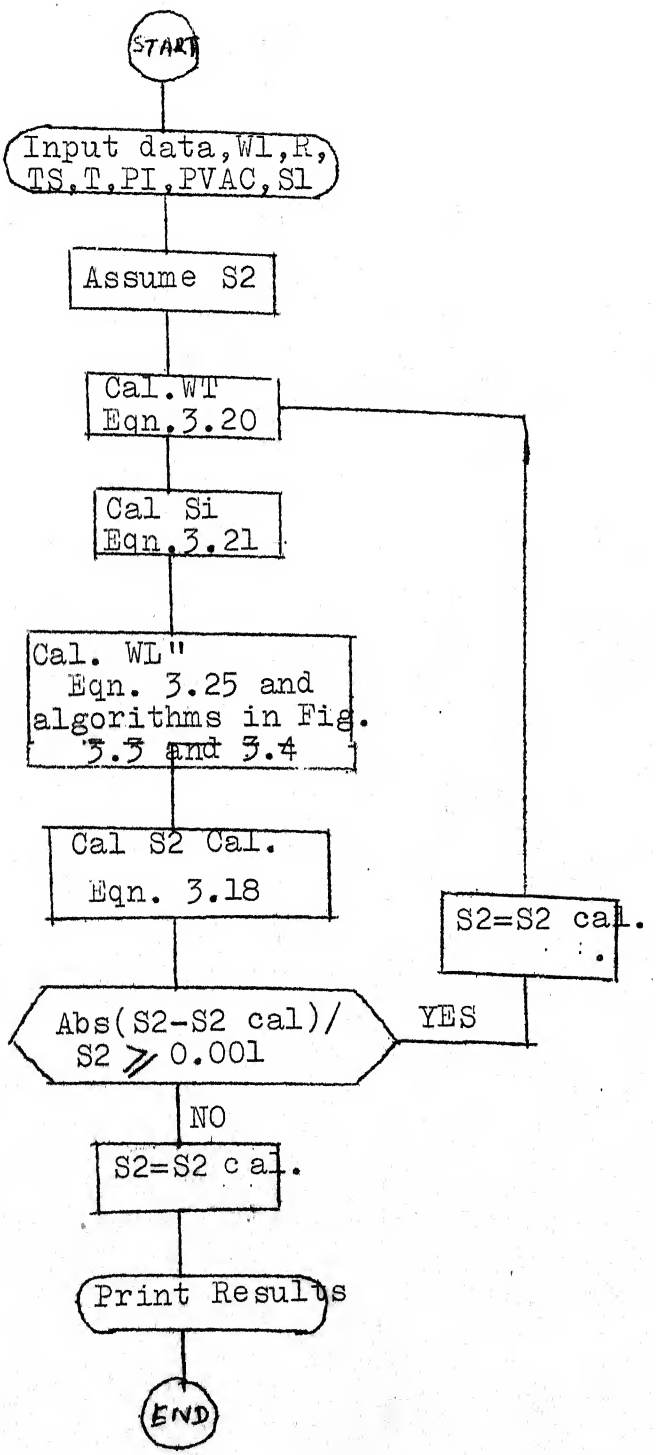

FIGURE 3.5 COMPUTATIONAL ALGORITHM FOR FLASH SEPARATOR

ratio, equations (3.19) to (3.21) are used to calculate total flow rate W_T and inlet liquor concentration to evaporator. Feed temperature and feed inlet pressure are known. With the given inlet conditions algorithms in Figure 3.3 and Figure 3.4 are used to determine liquor conditions and the end of tube. Liquor concentration after flashing is calculated using equations (3.25) and (3.18). Outlet liquor flow rate (W_L'') is calculated from equation (3.25). Liquor flow rate to flash separator (W_L'), and inlet liquor concentration are known. So outlet liquor concentration can be calculated from equation (3.18). Now the assumed value of S_2 and calculated value of S_2, S_{2cal} are compared. The calculated value is compared with the initial assumption (S_2) for convergence.

CHAPTER 4

RESULTS AND DISCUSSIONS

Computational schemes outlined in Figures 3.3 to 3.5 are used to simulate the evaporation process. The model is used for the following three cases:

1. Simulation of Badger's experimental data [10]
2. Simulation of forced circulation evaporation of kraft black liquor in a single vertical tube.
3. Simulation of forced circulation evaporation of kraft black liquor in a single vertical/horizontal tube with recirculation of liquor.

The results of the simulation studies for the above cases are discussed in the following sections.

4.1 Simulation of Badger's Experimental Data [10].

Badger and Brooks [10] have reported experimental data for boiling heat transfer obtained from a long tube vertical unit equipped with a single tube (L=6.1 m, 44.5/50.8 mm dia.) using water as the system. The above data include boiling length, evaporation rate, overall heat transfer coefficient and total heat transferred in boiling zone. Seventeen sets of data were drawn from Badger and Brooks' study and used in this investigation and are given

TABLE 4.1

BADGER'S EXPERIMENTAL DATA FOR THE EVAPORATION OF WATER IN LTV UNIT [10]

Serial No.	W_i kg/h	T_i °C	T_s °C	L_b m	E kg/h	U_b kW/m² K	$A_b Q_b$ kW
1	2	3	4	5	6	7	8
1(L-17)[a]	120.96	38.33	83.62	4.90	59.69	3.28	37.68
2(L-21)	111.60	50.57	81.63	5.12	54.59	3.25	34.74
3(L-22)	113.04	60.02	81.67	5.45	56.70	3.24	36.17
4(K-33)	112.30	61.80	98.30	5.48	73.48	3.48	47.54
5(M-16)	113.04	59.58	107.04	5.2	63.50	4.35	39.55
6(M-10)	114.48	86.52	106.84	5.51	66.86	4.34	41.84
7(L-18)	113.76	35.75	75.51	4.45	29.30	3.13	18.06
8(L-15)	114.48	39.30	79.13	4.90	41.00	3.72	25.65
9(L-13)	113.04	53.19	73.52	4.54	25.31	4.20	15.34
10(K-30)	210.96	74.86	98.58	5.69	81.46	3.69	50.92
11(L-12)	113.04	59.79	73.61	4.57	20.77	4.24	13.69
12(L-8)	116.28	59.91	76.57	5.24	38.96	3.56	24.68
13(K-42)	113.76	71.90	86.90	4.57	28.62	4.40	17.50

Table 4.1 (contd)

1	2	3	4	5	6	7	8
14(M-2)	113.04	58.38	104.42	4.57	43.90	4.26	27.51
15(M-13)	118.44	74.66	101.41	4.66	34.33	4.85	21.00
16(M-11)	116.28	87.24	101.31	4.84	34.20	4.78	20.74
17(K-32)	221.76	64.54	87.29	4.29	31.29	4.80	18.56

[a]Number in parenthesis indicate Badger's experimental data No.[10]

TABLE 4.2a:

COMPARISON OF BADGER'S DATA WITH SIMULATED RESULT

Sl. No.	Non-Boiling Zone		Boiling Zone						
	h_i cal.	U_{nb} cal.	h_i cal.	L_b,m			U_b		
				Obs.	Cal.	Percent Dev.	Obs.	Cal.	Percent Dev.
1	2	3	4	5	6	7	8	9	10
1	1.201	1.031	21.07	4.90	5.25	6.6	3.28	3.33	1.50
2	1.129	0.969	19.00	5.12	5.55	7.74	3.25	3.43	2.48
3	1.122	0.972	20.15	5.45	5.85	6.83	3.24	3.41	2.45
4	1.354	1.125	25.06	5.48	5.85	6.32	3.48	3.48	0.00
5	1.373	1.134	21.82	5.21	5.40	3.51	4.35	3.64	19.17
6	1.327	1.131	22.62	5.51	5.85	5.81	4.34	3.69	17.61
7	1.022	0.891	12.61	4.45	4.80	7.29	3.13	3.40	7.94
8	1.082	0.930	16.30	4.90	5.25	6.73	3.72	3.42	-8.77
9	0.973	0.873	6.86	4.54	4.95	8.28	4.20	3.28	27.76
10	1.572	1.281	25.57	5.69	5.85	2.73	3.69	2.75	34.30
11	0.941	0.846	8.30	4.57	4.95	7.67	4.24	3.36	26.19
12	1.023	0.908	11.12	5.24	5.55	5.58	3.56	3.43	3.75
13	1.090	0.965	8.706	4.57	4.95	7.67	4.40	3.44	-27.80

Table 4.2a (contd)

1	2	3	4	5	6	7	8	9	10
14	1.340	1.116	14.70	4.57	5.10	10.39	4.26	3.64	17.01
15	1.288	1.098	11.60	4.66	4.95	5 .85	4.85	3.48	39.22
16	1.198	1.051	11.26	4.84	4.80	-0.96	4.78	3.39	-40.90
17	1.408	1.184	10.16	4.29	3.60	-19.30	4.80	3.18	-50.98

h_i, U_{nb}, U_b - kW/m^2 K

TABLE 4.2b

COMPARISON OF BADGER'S DATA WITH SIMULATED RESULT

Sl. No.	E(kg/h) Obs.	E(kg/h) Cal.	Percent Dev.	A_bQ_b (kW) Obs	A_bQ_b (kW) Cal.	Percent Dev.
1	59.69	80.10	25.48	37.68	50.32	25.12
2	54.79	67.75	19.12	34.74	42.53	18.31
3	56.70	76.15	25.54	36.17	47.16	23.30
4	73.48	100.43	26.88	47.54	62.96	24.49
5	63.50	73.39	13.47	39.55	47.66	17.01
6	66.86	79.70	16.11	41.84	48.67	14.03
7	29.30	30.20	2.98	18.00	18.94	4.96
8	41.00	52.99	22.62	25.65	33.76	24.02
9	25.31	21.18	-19.49	15.34	13.24	-15.86
10	81.46	166.94	51.20	50.92	101.45	49.80
11	20.77	23.21	10.51	13.69	14.37	4.73
12	38.96	47.98	18.79	24.68	29.79	17.15
13	38.62	26.23	-47.23	17.50	15.52	-14.98
14	43.90	49.73	11.72	27.51	30.07	8.51
15	34.33	37.54	8.55	21.00	21.47	2.18
16	34.20	37.08	8.65	20.74	21.43	3.21
17	31.29	41.46	24.52	18.56	17.35	-6.97

I.I.T. KANPUR
CENTRAL LIBRARY
Acc. No. A 58350

in Table 4.1. Numbers in parentheses correspond to original serial number in Badger and Brooks' experimental data. The length of differential section (dz) was taken as 15 cm for the computation. The feed was below saturation temperature in all the cases giving both non-boiling and boiling zones. The length of non-boiling zone was predicted using equations (2.3) to (2.5), (2.7) to(2.9), (3.3) and (3.10) by stepwise computation till the maximum in temperature profile was obtained. Average values of film heat transfer coefficient and overall heat transfer coefficient were calculated from $h_{inb} = \sum h_{inb} * \Delta T_i / \sum T_i$ and $U_{nb} = \sum U_i * \Delta T_i / \sum T_i$. Subsequent calculations based on equations (2.6), (2.10), (3.10), (3.12), (3.15) gave liquid film, overall heat transfer coefficients, evaporation rate and total heat transferred in boiling zone. Table 4.2a and 4.2b give a comparison of the above results with Badger and Brooks' experimental observations. The results show very good agreement of predicted length of non-boiling zone with the observed values with an average 5 per cent deviation. Predicted values of overall boiling heat transfer coefficient, evaporation rate and total heat transferred in boiling section show average deviations of 13, 13 and 12 per cent respectively. Earlier simulation study by Agarwal [9] has also considered some of the results of Badger's and Brooks. The average deviations obtained in this study and values reported by Agarwal [9] are given below.

Variable	Deviation, Per cent	
	This Study	Agarwal [9]
L_b(m)	5	15
U_b(kW/m^2 K)	13	13
E(kg/h)	13	13
$A_b Q_b$	12	17

The above values show a better agreement of the prediction of this study with Badger's observations. Liquid film heat transfer coefficient in non-boiling zone is predicted in this work by Eubank and Proctor [30] equation for the viscous region which includes Grashoff number to account for the effect of natural convection. Agarwal has used an empirical correlation [40] for estimating the overall heat transfer coefficient in non-boiling zone which leads to reported 15 per cent average deviation for the length of non-boiling zone. Table 4.3 shows comparison of Badger's result with Agarwal's result.

Heat transfer coefficients for boiling in Agarwal's[9] model are based on Coulson-McNelly and Penman-Tait [11,14] correlations for the nucleate and annular film boiling regions respectively. Schrock-Grossman correlation for forced convection boiling is used in this study to predict film heat transfer coefficient for the entire boiling zone. The two models predict Badger's data equally well as observed from

TABLE 4.3

COMPARISON OF BADGER'S DATA WITH AGARWAL'S [9] RESULT

Sl. No.	L_b (m)			U_b (kW/m^2 K)			E(kg/h)			$A_b Q_b$ (kW)		
	Obs.	Cal.	Percent Dev.	Obs.	Cal.	Percent Dev.	Obs.	Cal.	Percent Dev.	Obs	Cal.	Percent Dev.
1	4.91	4.04	-19.5	3.34	2.72	-18.3	59.5	48.8	-17.5	37.5	30.94	-18.0
2	5.12	4.25	-17.1	3.25	2.79	-14.1	54.6	44.1	-18.9	34.6	28.40	-16.9
3	5.45	4.58	-16.2	3.24	2.78	-14.2	56.5	46.0	-18.4	35.6	28.95	-20.2
4	4.58	4.99	- 7.3	3.49	2.71	-22.2	73.4	66.5	- 8.9	47.55	42.40	-11.1
7	5.54	3.59	-19.6	3.13	2.76	-11.6	29.3	33.4	14.8	18.10	21.20	16.4
18	5.65	5.42	- 4.1	3,26	2.68	-17.5	75.0	68.3	- 8.5	47.80	43.90	-8.6
19	5.19	4.21	-18.8	3.45	2.76	-20.0	43.4	40.0	- 7.6	27.62	25.77	-6.8

S.No.18 and 19 correspond to K-38 and K-45 of Badger's data [10]

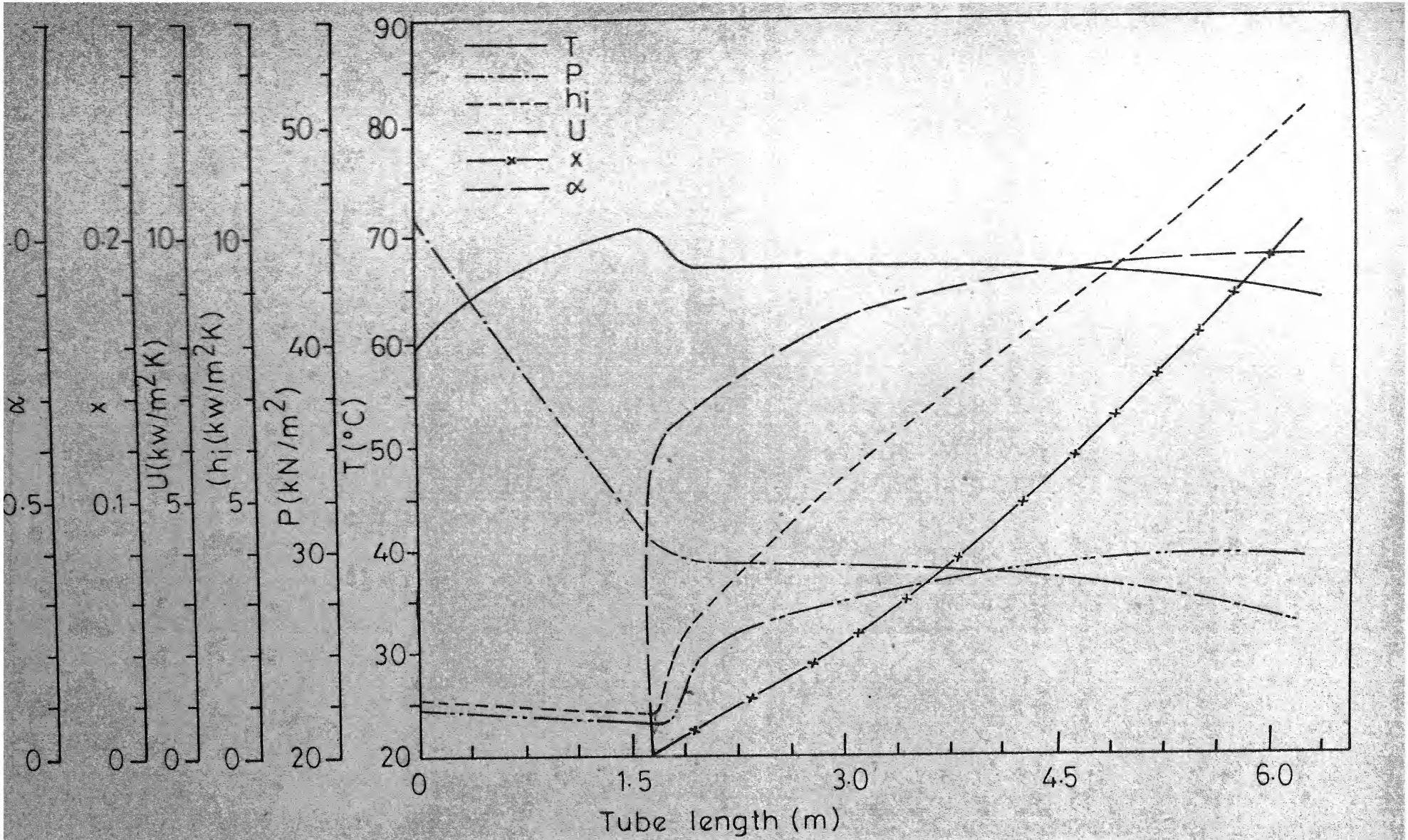

Fig. 4.1 - Predicted longitudinal profiles of pressure (P), temperature (T), film coefficient (h_i), overall heat transfer coefficient (U), quality (x), void fraction (α). Badger's data [L-12].

TABLE 4.4

SIMULATION RESULTS FOR BADGER'S EXPERIMENTAL DATA

Sl. No.	Temp., °C		Pressure, kN/m²		Quality	Void fraction	Boiling Zone			
	Feed	Max	Feed	Sat.	Exit	exit	h_{il}	h_{i2}	U_1	U_2
1	38.3	72.0	42.0	29.7	0.66	0.99	0.926	31.73	0.825	3.37
2	50.5	71.4	40.0	30.5	0.60	0.99	0.862	27.98	0.778	3.50
3	60.0	71.7	36.8	30.2	0.66	0.99	0.852	29.70	0.770	3.45
4	61.8	83.7	64.5	57.8	0.79	0.99	0.934	39.30	0.840	3.52
5	59.5	96.7	104.5	93.4	0.658	0.99	0.814	33.60	0.747	3.85
6	86.5	98.5	101.5	94.8	0.696	0.99	0.773	34.74	0.715	3.88
7	37.7	67.1	46.5	29.7	0.265	0.97	0.779	15.14	0.718	3.82
8	39.3	68.9	42.1	29.7	0.462	0.99	0.848	22.80	0.768	3.58
9	53.1	69.2	45.6	30.3	0.186	0.96	0.707	11.48	0.659	3.85
10	74.8	84.9	62.8	56.1	0.791	0.99	1.082	45.05	0.955	2.69
11	59.7	70.5	45.3	30.0	0.205	0.96	0.690	12.22	0.648	3.86
12	59.9	70.3	48.9	29.3	0.412	0.98	0.770	20.20	0.709	3.61
13	71.9	84.2	73.3	58.03	0.230	0.96	0.663	15.21	0.630	3.85
14	58.3	97.4	110.5	96.7	0.463	0.98	0.758	25.13	0.706	3.98
15	74.4	97.3	110.2	94.9	0.317	0.97	0.680	21.12	0.643	3.70
16	87.24	97.5	107.9	96.9	0.318	0.976	0.654	20.47	0.618	3.79
17	64,54	82.5	75.9	53.4	0.186	0.974	0.918	17.45	0.842	3.06

the average deviations for the value of boiling length, overall heat transfer coefficient, evaporation rate and total heat transferred in boiling zone.

A summary of the simulation results of this study using Badger's experimental data is given in Table 4.4. Table 4.4 shows temperature and pressure of the fluid at the inlet, end of non-boiling zone and exit of the tube, quality and void fraction of vapor liquid mixture at exit and liquid film and overall heat transfer coefficients in boiling zone. A typical set of profiles for temperature, pressure, quality, film and overall heat transfer coefficients are given in Figure 4.1. for data set 11. Temperature profile shows a maximum of 70.5°C at 1.65 m indicating completion of non-boiling zone, this is accompanied by a rapid reduction in pressure caused by decrease in hydrostatic head. The values of film and overall heat transfer coefficient are nearly constant at 1.05 and 0.90 respectively. The start of boiling zone is evident from Figure 4.1, from the profiles of quality, and heat transfer coefficients as depicted by the graphs in Figure 4.1. These profiles are similar to the results obtained by Agarwal. Thus both the models satisfactorily predict Badgers and Brooks experimental data.

4.2 Simulation of Forced Circulation Evaporation in a Single Vertical Tube:

The effect of various operational parameters like feed temperature, feed liquor concentration, feed rate on performance of a single tube of 6 m long vertical evaporator is studied using the simulation programme. Even though in commercial practice evaporator units consists of 200-500 tubes (single pass) in the calendria, in this work, a single tube is considered for simulation purposes. The single tube is assumed to be a typical one representing fluid flow and heat transfer mechanisms encountered in a full scale unit. It is assumed that liquor is distributed equally in all the tubes, and that the various process conditions are identical for all the tubes. A dirt scale resistance R_D = 0.45 m^2 K/kW is assumed.

In this study, black liquor is taken as the process liquor, because the necessary correlations for engineering properties for various commercial samples [36,37] are readily available. Further forced circulation evaporator units are increasingly used for the viscous concentration range of 55-65 per cent.

4.2.1 Effect of Feed Liquor Concentration on Performance:

Feed liquor concentration of bamboo kraft black liquor is varied from 35 to 65 per cent, while keeping the feed temperature and rate constant at 100°C and 10 kg/s/tube. The

latter corresponds to a tube velocity 3.5 - 4.0 m/s. Simulation results of Table 4.5 show that the overall heat transfer coefficient falls with increase in feed liquor concentration which contributes to a higher viscosity. Viscosity of liquor increases 2.5 cp for 35 per cent to 48 cp for at 60 per cent concentration (at 100°C) with a decrease in N_{Re} from 10×10^4 to 0.5×10^4. Figure 4.2 shows the profiles of non-boiling and boiling overall heat transfer coefficients with liquor concentration as the parameter. Figure 4.3 shows average film heat transfer coefficients for non-boiling and boiling zones and overall heat transfer coefficient decrease with increase in viscosity of feed. Pressure profiles along the tube are depicted in Figure 4.4 with feed concentration a s parameter show that increasing feed viscosity pressure at the tube end is lower. Effect of feed liquor concentration, feed liquor temperature and feed rate on total pressure drop is given in Figure 4.5. Total pressure drop as depicted in Figure 4.5 increases with the viscosity of the feed. The results in Table 4.5 also show that change in liquor concentration is very small (less then 1.0 percent) and this necessiates the use of recycle concept to achieve the desired concentration levels.

4.2.2 Effect of Feed Temperature on Performance:

The effect of temperature of bamboo kraft black liquor (45 per cent) was studied at 90 to 110°C and the predicted

TABLE 4.5

EFFECT OF CONCENTRATION OF FEED ON THE PERFORMANCE OF SINGLE TUBE FCE (VERTICAL)

Evaporator: L = 6m D = 5.03/5,43 cm n = 1 N=1

Process Conditions:

System: Bamboo Kraft Black Liquor

P_i = 157 kN/m^2 T_i = 100^{o}C W_i = 2.5 kg/s R_D = 0.17 m^2 ^{o}K/kW

T_s = 140^{o}C R = 0

S_i percent	μ cp	u m/s	N_{Re}	T_{max}	ΔP kN/m^2	S_o percent	L_b m	U_{nb} W/m^2 K	U_b W/m^2 K	U W/m^2 K	h_{inb} W/m^2 K	h_{ib} W/m^2 K
35	2.48	4.00	101726	101.7	71.7	35.14	1.4	2055	2124	2017	8585	10880
40	4.87	3.88	51919	101.6	74.9	40.16	1.4	1876	1984	1901	5645	7446
45	5.33	3.77	47443	101.6	76.7	45.16	1.3	1896	1937	1904	5900	6935
50	10.98	3.67	23063	101.4	80.6	50.20	1.3	1646	1757	1670	3685	4661
55	22.93	3.57	11044	101.2	83.9	55.21	1.3	1406	1526	1432	2539	3140
60	47.88	3.48	5288	101.0	88.3	60.20	1.4	1143	1413	1207	1747	2657

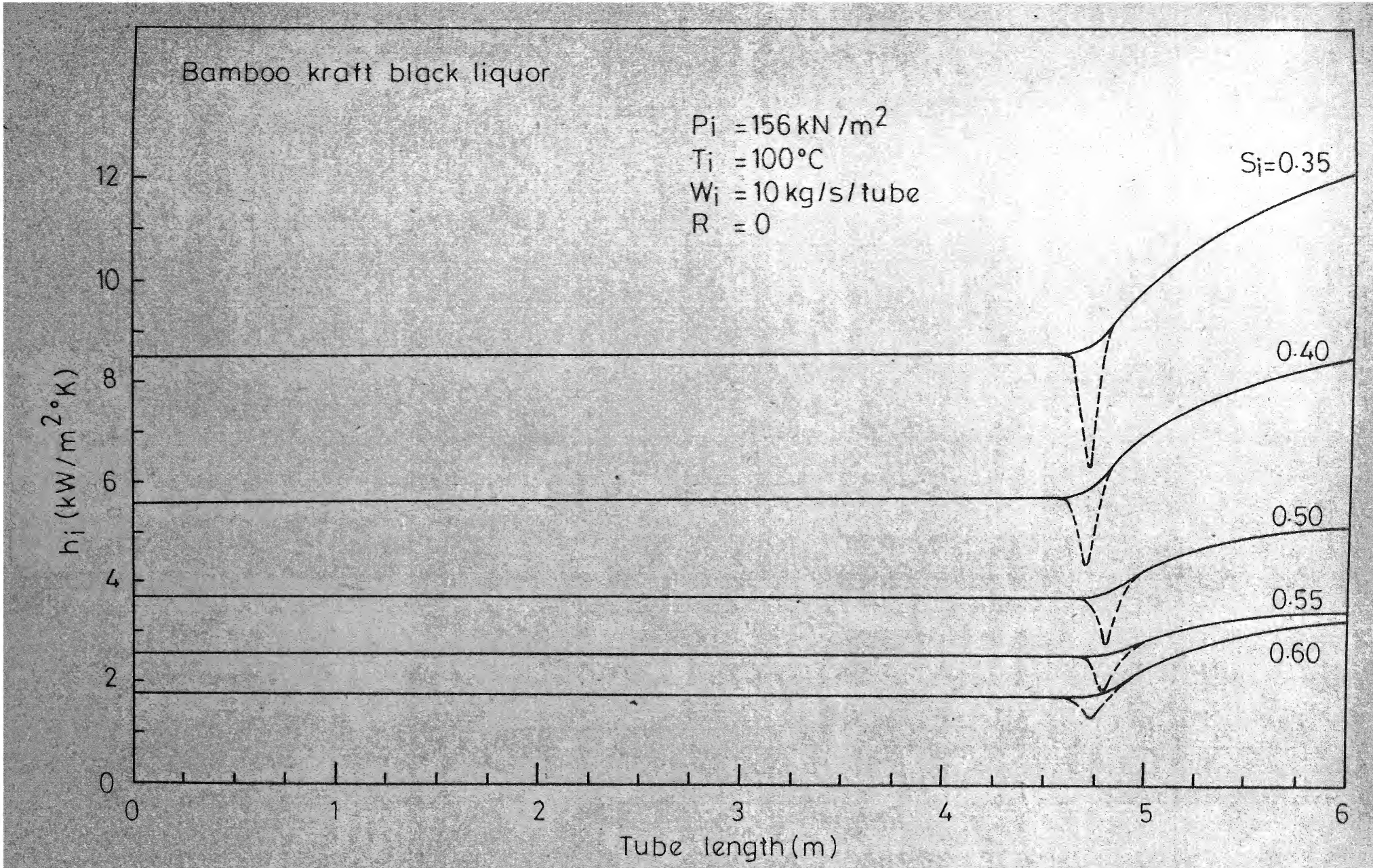

Fig 4.2 - Effect of feed concentration (S_i) on predicted profile of film heat transfer coefficient.

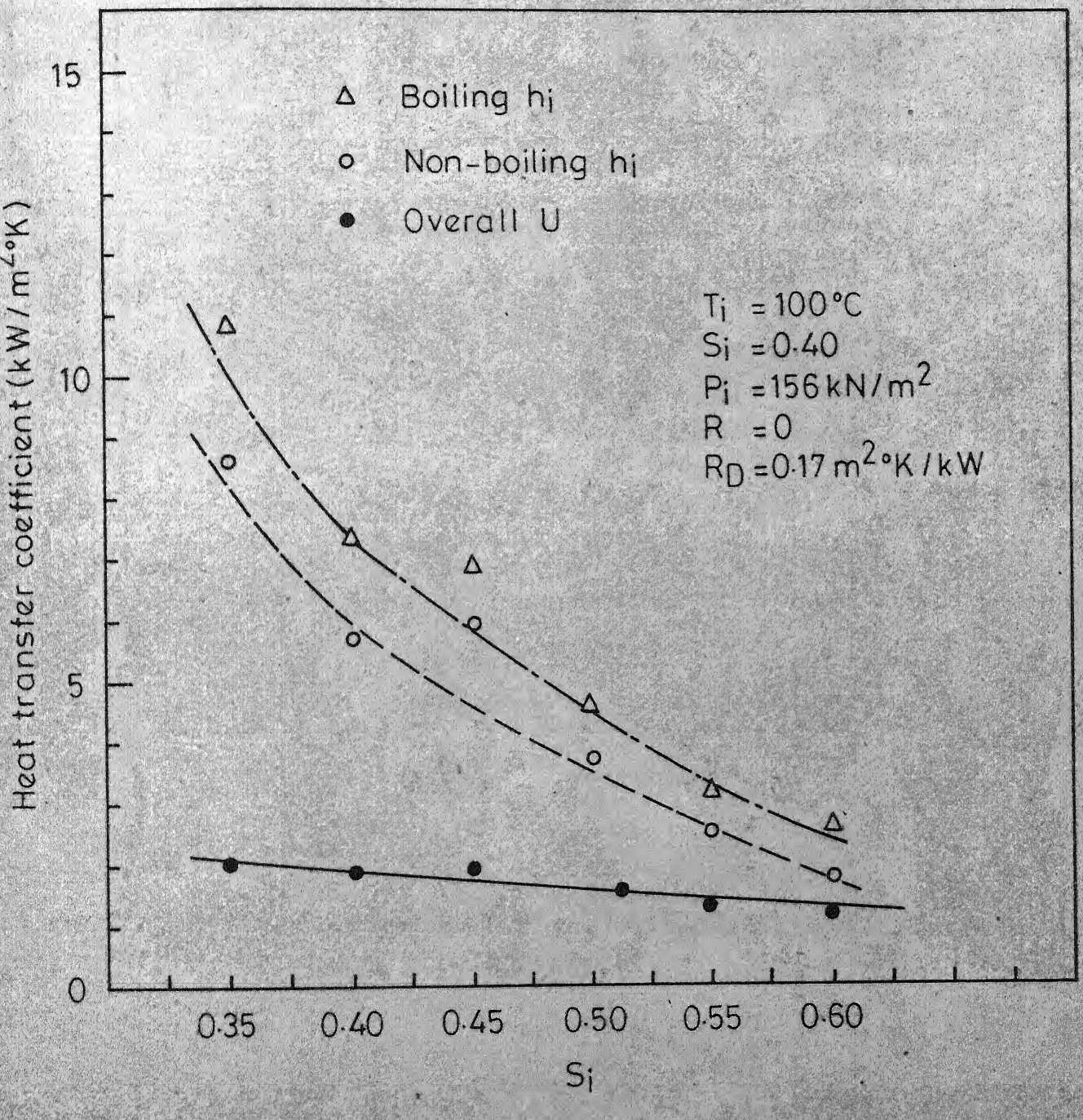

Fig. 4·3 - Effect of feed liquor concentration (Si) on predicted heat transfer coefficient.

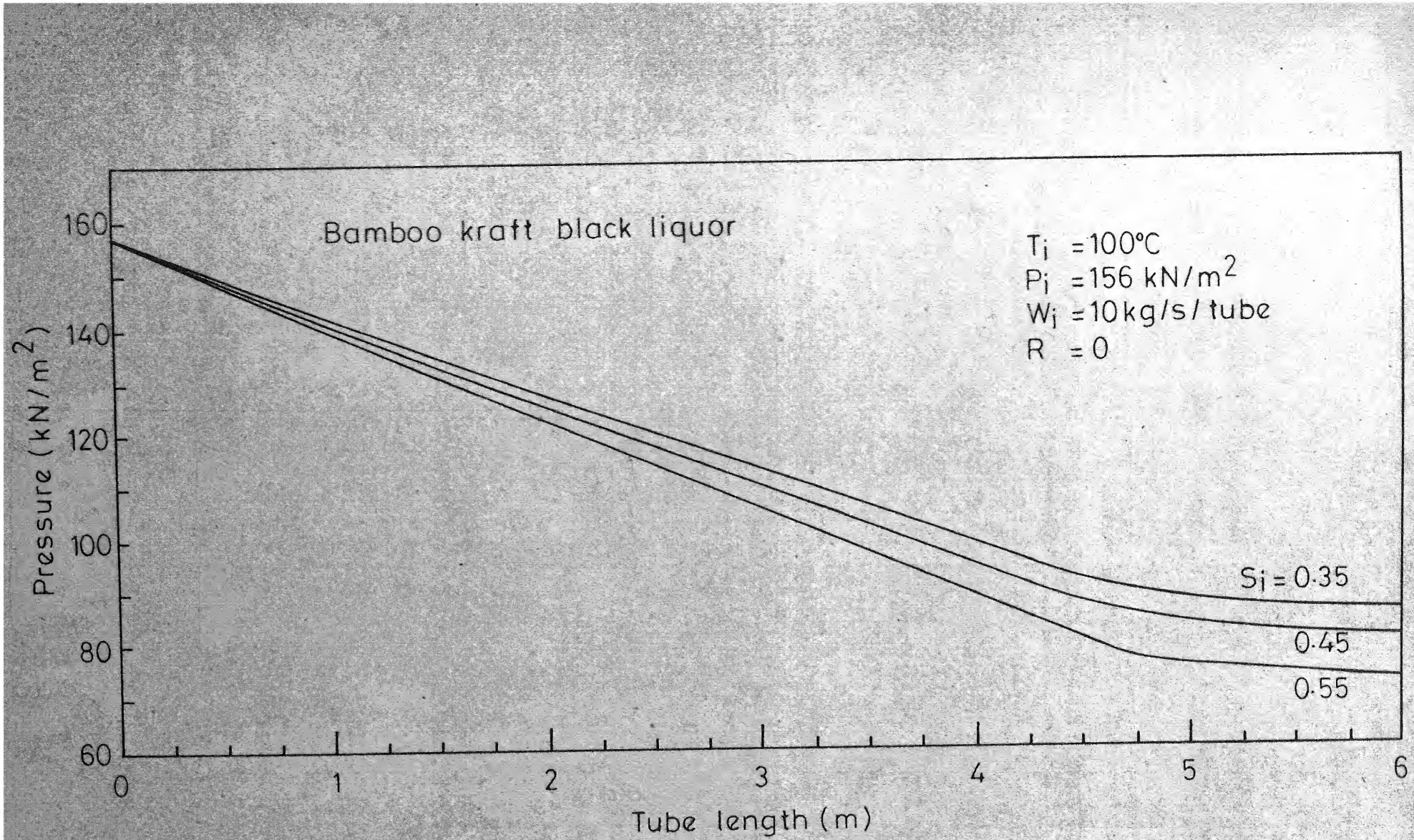

Fig. 4.4 – Effect of concentration (Si) on predicted profile of pressure (P).

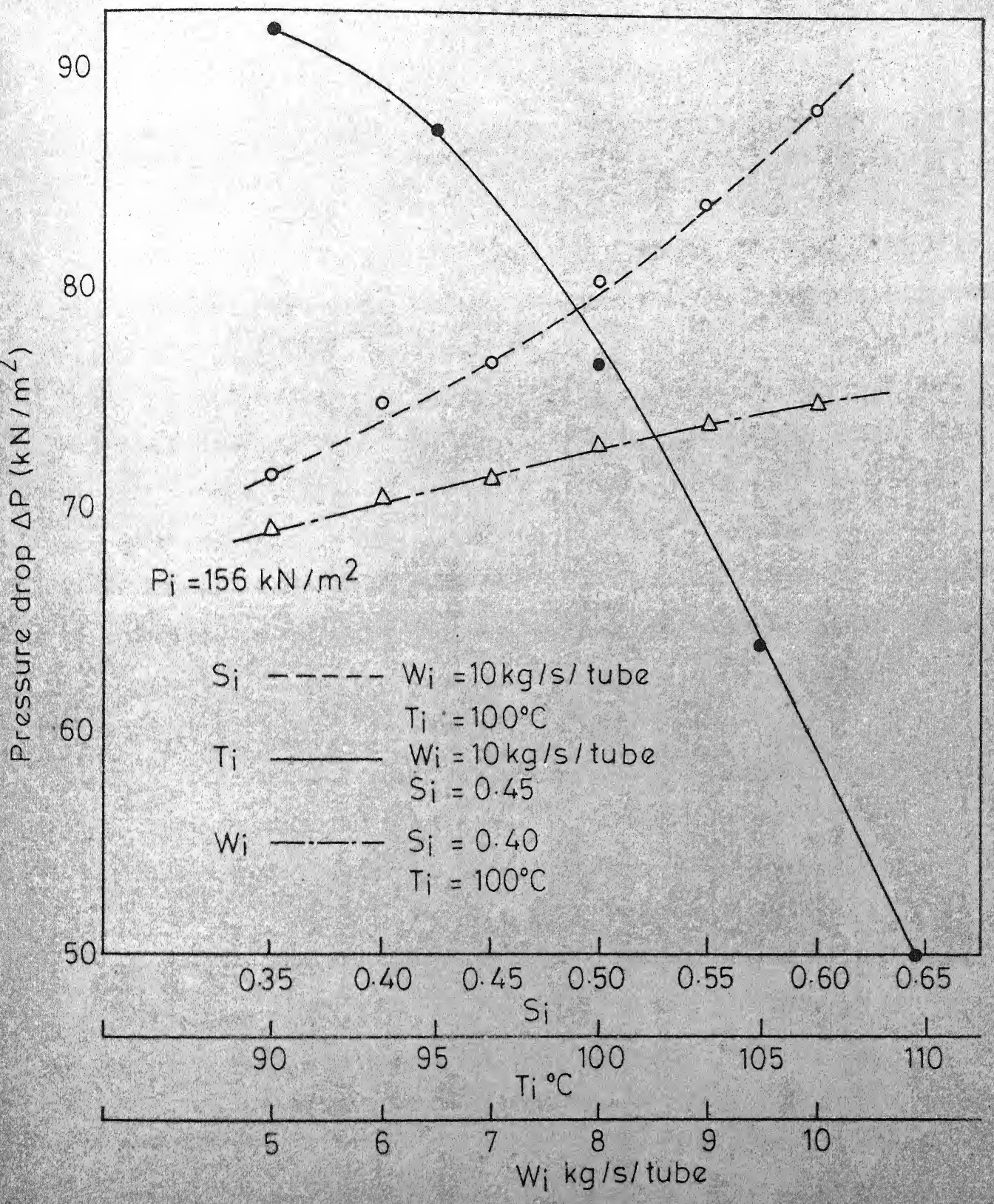

Fig. 4·5 - Effect of feed rate (Wi), feed temperature (Ti), feed liquor concentration (Si) on pressure drop (Δ P).

results are summarised in Table 4.6. The results show an increase in overall heat transfer coefficient and decrease in pressure drop with feed temperature. Figure 4.6 shows profiles of tube side film coefficient for various feed temperatures. There is a discontinuity in the profile during transition from non-boiling to boiling zone. Film coefficient for boiling zone slightly falls below non-boiling zone and then rises. Film heat transfer coefficient for boiling zone is always higher than film heat transfer coefficient in non-boiling zone. This slight discontinuity can be due to failure of Schrock-Grossman correlation to predict film heat transfer coefficient during transition from non-boiling to boiling region. Schrock-Grossman correlation is developed on the basis of data for fully developed boiling zone.

Figure 4.7 shows an increase in average film heat transfer coefficients for both non-boiling and boiling zones. This is due to the fact that feed liquor concentration remaining same feed liquor viscosity falls with rise in feed temperature and consequently inlet Reynold's number increases. Overall heat transfer coefficients also improves due to increase in the individual heat transfer coefficients.

Table 4.6 shows that liquor concentration at the exit of the tube increases with increase in feed liquor temperature. Figure 4.8 shows the concentration profiles with feed temperature as parameter. Increase in liquor concentration at the

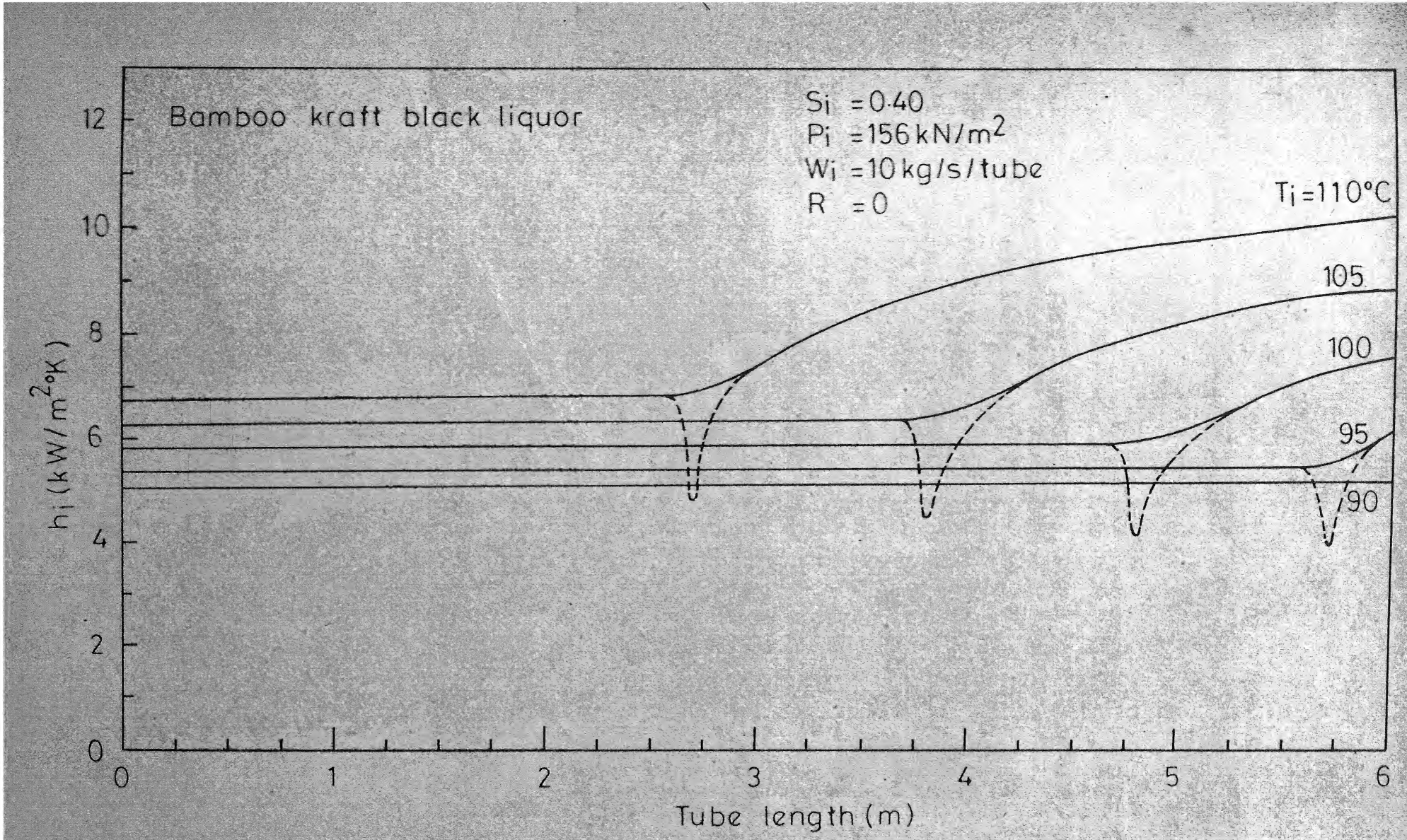

Fig 4·6 - Effect of feed temperature (T_i) on predicted profile of film heat transfer coefficient

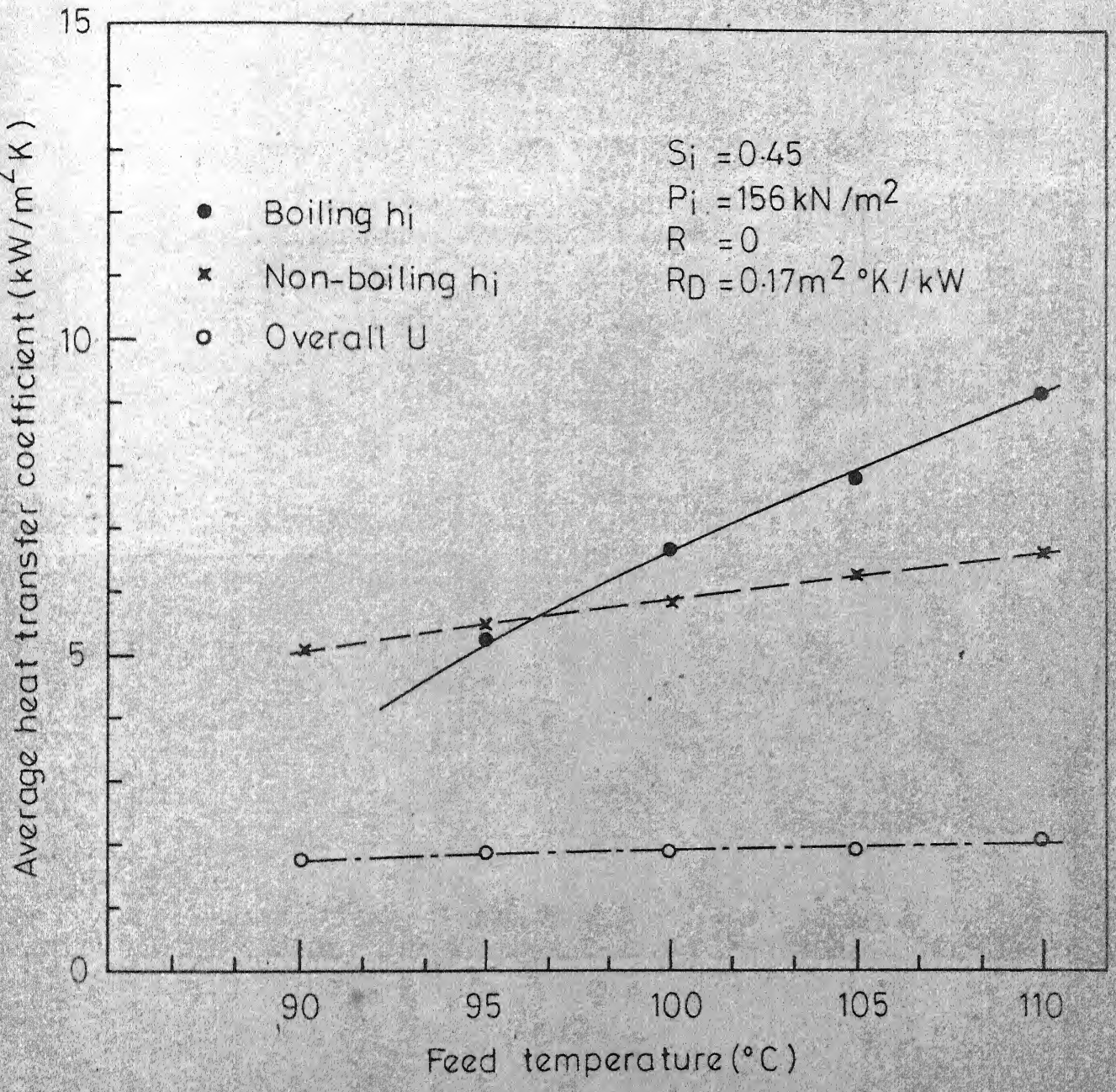

Fig. 4.7 - Effect of feed liquor temperature (T_i) on predicted heat transfer coefficient.

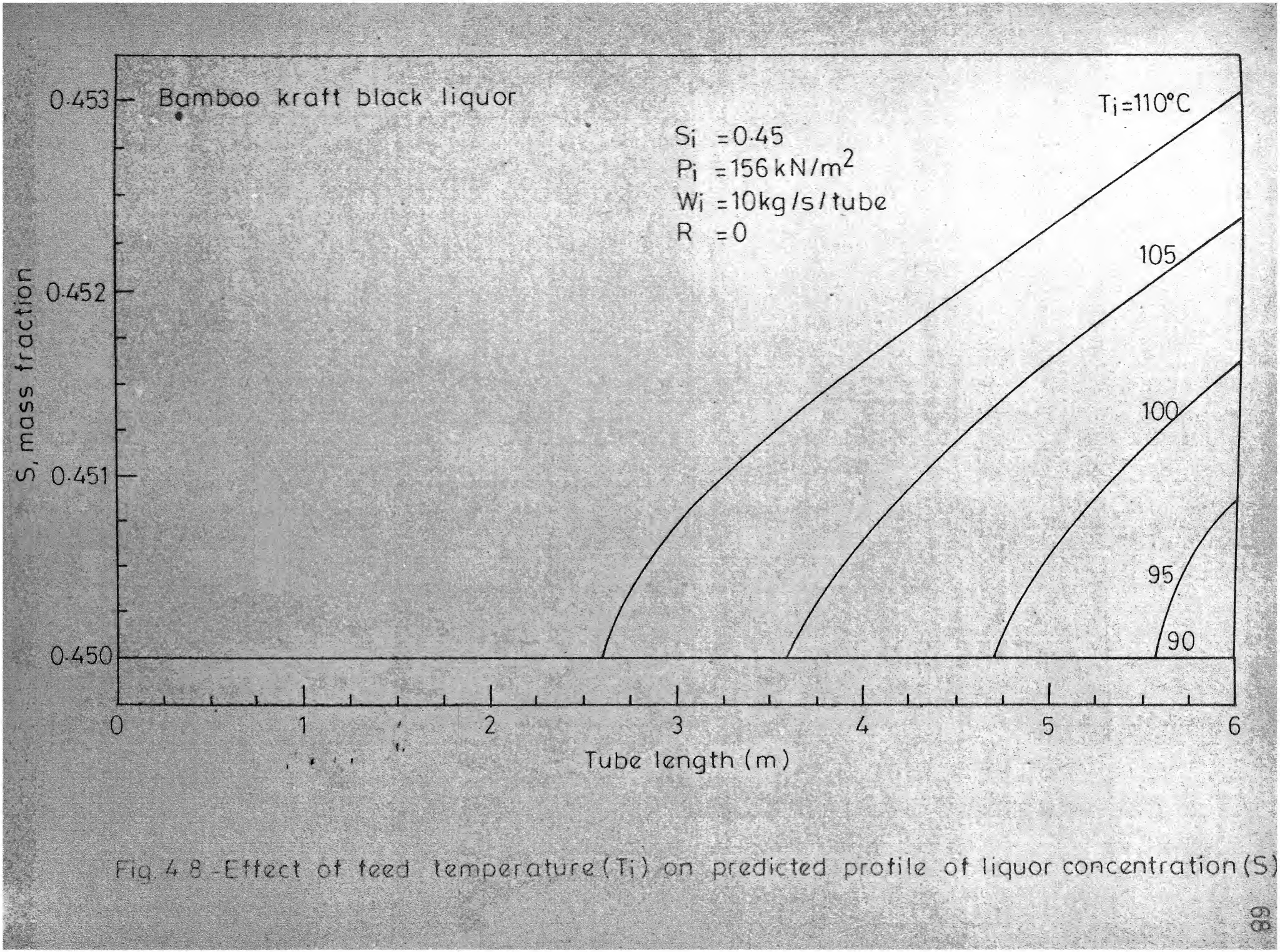

Fig. 4.8 - Effect of feed temperature (Ti) on predicted profile of liquor concentration (S)

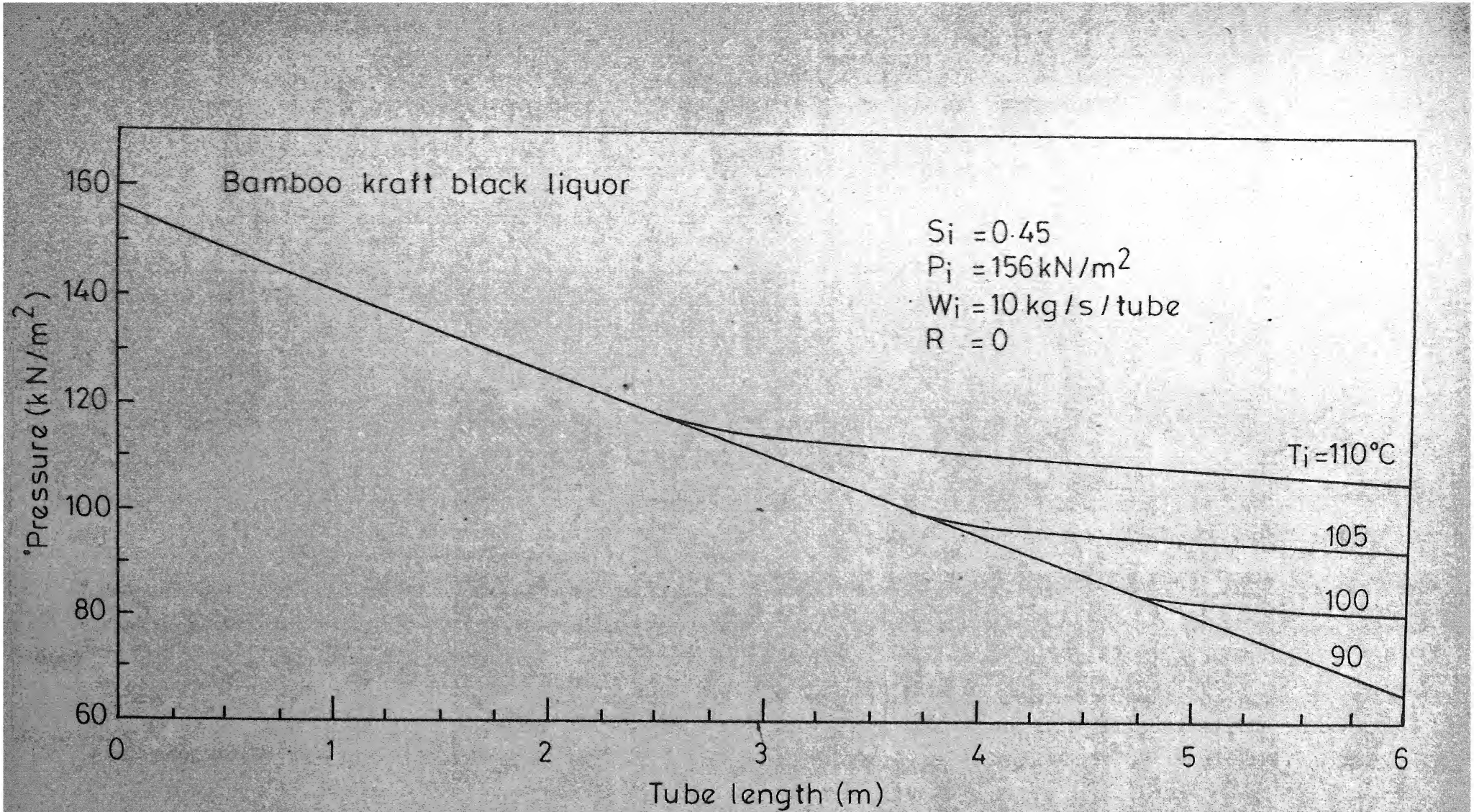

Fig. 4.9 - Effect of feed temperature (Ti) on predicted profile of pressure (P).

TABLE 4.6

EFFECT OF FEED TEMPERATURE ON PERFORMANCE OF SINGLE TUBE FORCED CIRCULATION EVAPORATOR(VERTICAL)

Evaporator: L = 6 m, D = 5.03/5.43 cm n = 1, N = 1

Process Conditions:

System: Bamboo Kraft Black Liquor

P_i = 157.kN/m^2 S_i = 45 per cent W_i = 10 kg/s/tube

R_D = 0.17 m^2 K/kW T_s = 145^{o}C R = 0

T_i ^oC	μ cp	u m/s	N_{Re}	T_{max} ^oC	ΔP kN/m^2	S percent	L_b m	U_{nb} W/m^{2}K	U_b W/m^2 K	U W/m^2 K	h_{inb} W/m^2 K	h_{ib} W/m^2 K
90.0	7.66	3.76	33043	-	91.65	45.00	-	1770	-	1770	5100	-
95.0	6.38	3.77	39686	97.11	87.49	45.008	0.4	1832	1806	1830	5495	5300
100.0	5.33	3.77	47443	101.63	76.74	45.164	1.3	1895	1937	1904	5900	6770
105.0	4.88	3.78	56460	106.15	64.18	45.235	2.3	1966	2037	1994	6330	7970
110.0	3.78	3.78	66900	110.72	49.93	45.306	3.4	2043	2133	2095	6780	9200

exit is due to the fact that with increase in feed temperature, boiling length increases and more vaporization takes place inside the tube. For a feed temperature of 90°C there is no boiling section and liquor concentration remains unchanged. For a feed temperature of 110°C the boiling length is 3.4 m and concentration rises by 0.3 per cent. Figure 4.9 shows pressure profile along tube length indicating that with increase in feed temperature boiling length increases ar Figure 4.5 shows a marked fall in pressure drop with increase in feed liquor temperature. This is due to fall in viscosity of the feed liquor with increase in feed temperatures.

4.2.3 Effect of Feed Liquor Rate on Performance:

Feed liquor rate of black liquor was varied from 5 to 10 kg/s/tube, while feed liquor concentration was kept fixed at 40 per cent and feed temperature at 100°C.

Table 4.7 summarises the predicted results. Figure 4.10 shows profiles of tube side film coefficient for various feed rates. Slight discontinuity in the film coefficient has been explained in Sec.4.2.2. Figure 4.11 depicts effect of feed rate on average heat transfer coefficients. Table 4.7 shows 10 per cent increase in heat transfer coefficients and 15 per cent increase in pressure drop for a two fold increase in feed rate.

TABLE 4.7

EFFECT OF FEED RATE ON PERFORMANCE OF SINGLE TUBE FORCED CIRCULATION EVAPORATOR(VERTICAL)

Evaporator: L = 6 m D = 5.03/5.43 cm n = 1, N =1,

Process Conditions:

System:Bamboo Kraft Black Liquor

P_i = 157 kN/m^2 S_i = 40 per cent T_i = 100^{o}C T_s = 145^{o}C

R = 0 R_D = 0.17 m^2 K/kW μ = 4.87 cp

W_i kg/s	u m/s	N_{Re}	T_{max} ^oC	ΔP kN/m^2	L_b m	U_{nb} W/m^2 K	U_b W/m^2 K	U W/m^2 K	S per^{o}cent	h_{inb} W/m^2 K	h_{ib} W/m^2 K
5.0	1.94	25959	102.75	69.18	1.1	1574	1768	1609	40.134	3260	4680
6.0	2.33	31151	102.43	70.54	1.1	1662	1828	1692	40.135	3760	5290
7.0	2.71	36343	102.13	71.38	1.2	1731	1861	1757	40.131	4260	5540
8.0	3.10	41535	101.93	72.86	1.2	1783	1919	1810	40.145	4730	6430
9.0	3.49	46727	101.73	73.83	1.3	1832	1951	1858	40.152	5190	6900
10.0	3.88	51919	101.56	74.9	1.4	1875	1984	1901	40.160	5650	7440

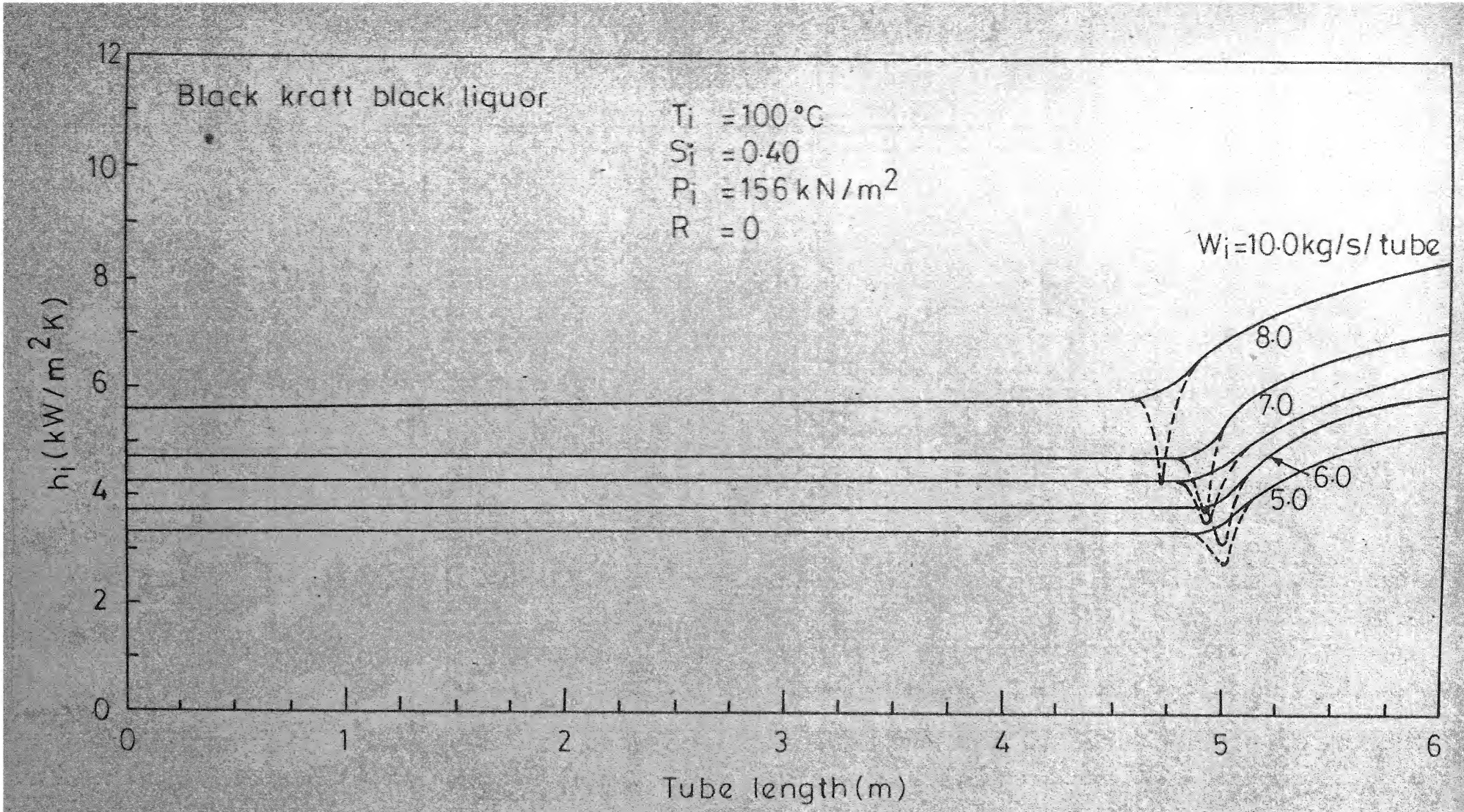

Fig. 4.10- Effect of feed rate (W_i) on predicted profile of film heat transfer coefficient.

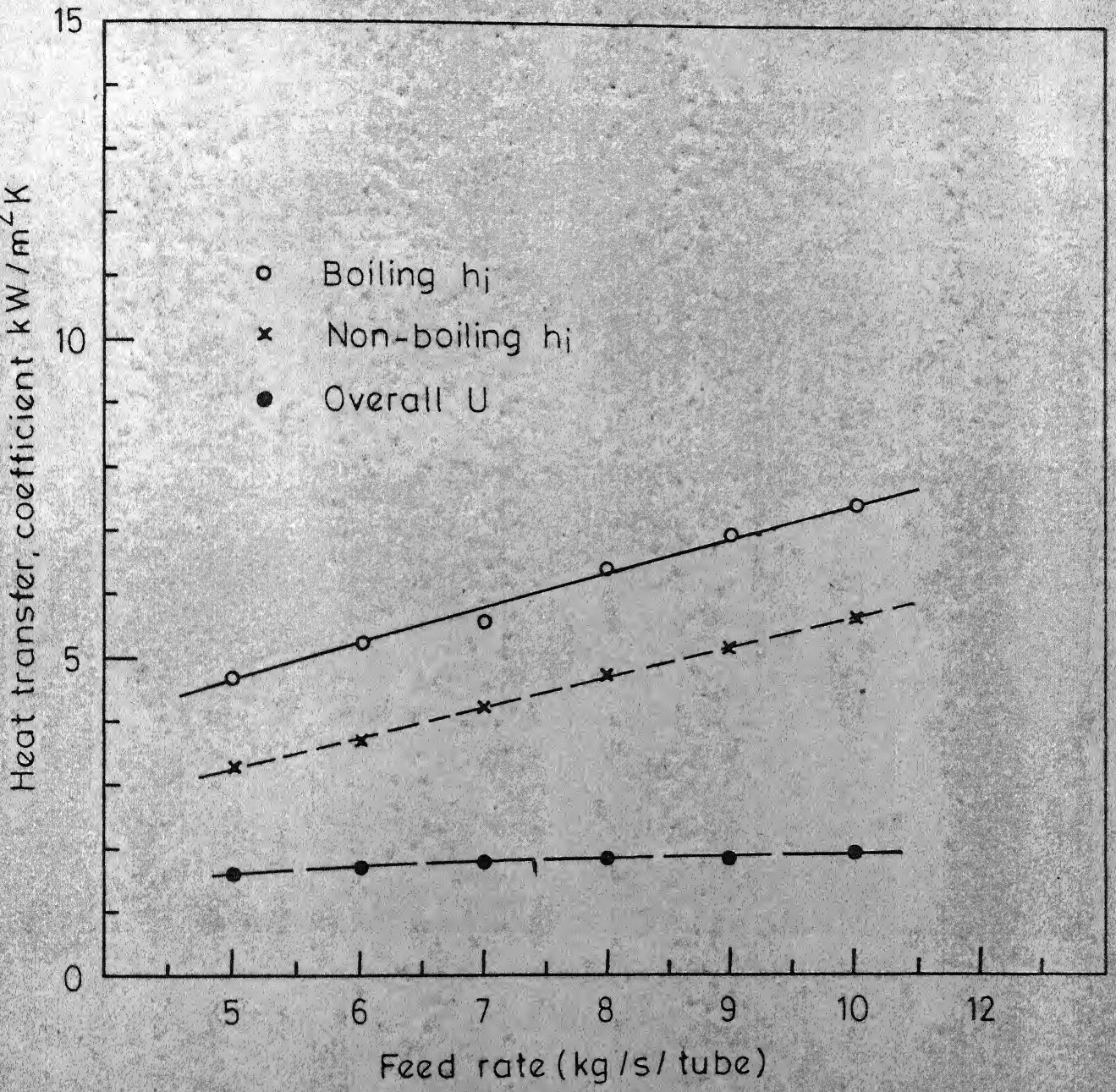

Fig. 4.11- Effect of feed rate (W_i) on predicted heat transfer coefficient.

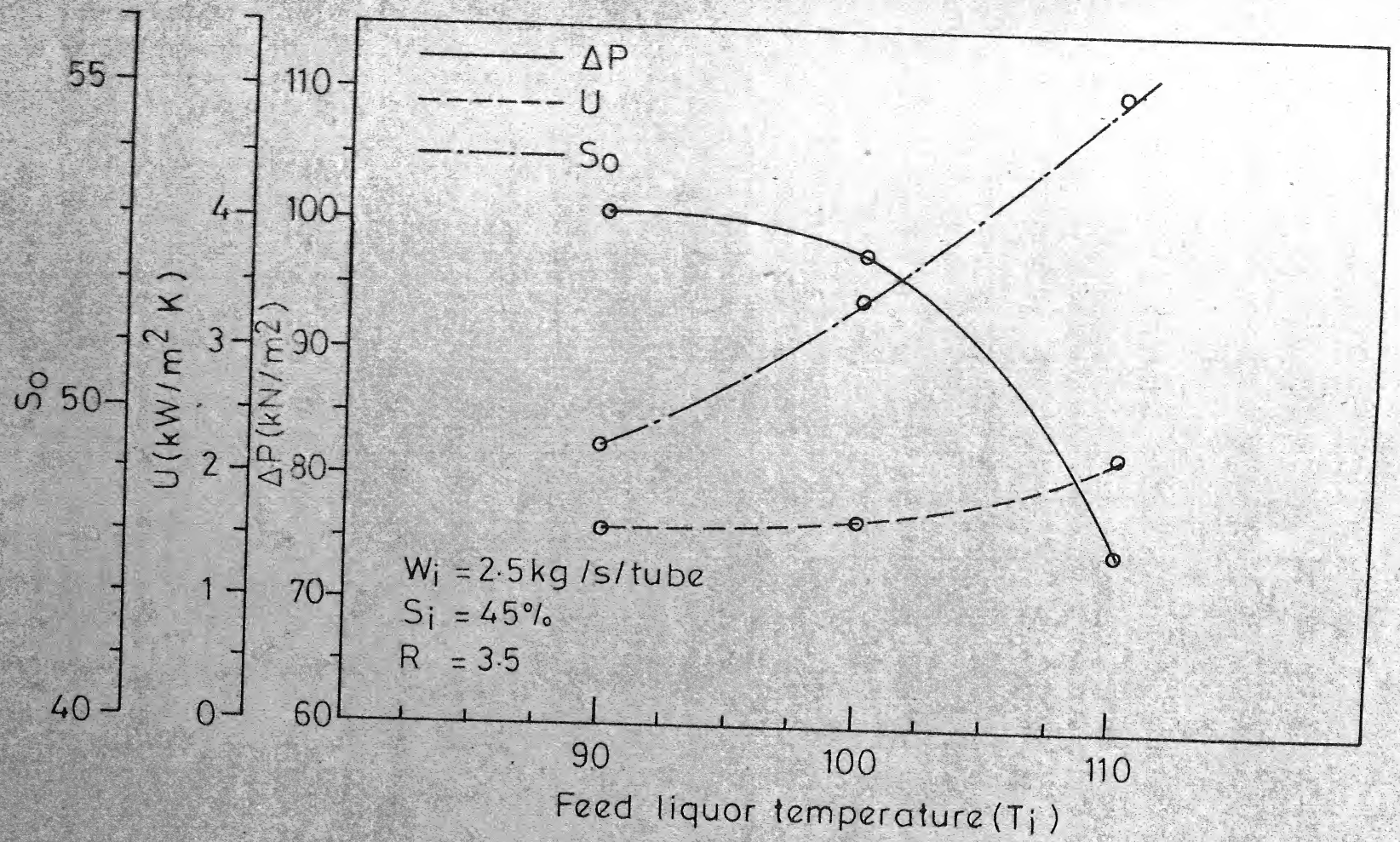

Fig 4.12 - Effect of feed liquor temperature (T_i) on performance of FCE (vertical calendria).

4.3 Simulation of Forced Circulation Evaporation with Recycle:

Concentration rise per pass in a FCE unit without recycle is very small (less than 1.0 per cent), hence to achieve higher concentration of the product liquor, part of the product is recycled. A commercial FCE unit normally 2-6 passes and 100-200 tubes/pass. An evaporator consisting of three passes and one tube/pass is considered. An evaporator consisting of three passes and one tube per pass is considered in this work. Effect of feed liquor temperature, feed liquor concentration and recycle ratio on performance are studied using simulation programme. Results for vertical and horizontal orientations of the calendria are compared. Kraft black liquor is taken as the process liquor. Vacuum in the vapor space is assumed to be constant at 35 kN/m^2.

4.3.1 Effect of Feed Temperature on Performance:

Feed temperature is an important process variable in evaporator operation and determines effective utilization of the available heat transfer surface for evaporation duty. Feed temperature of inlet liquor is varied (90, 100, 110°C) keeping other parameters constant to study change in performance. The values of feed concentration, recycle rate, and separator pressure are kept constant. Tables 4.8 and 4.9 summarises the results for FCE with vertical and horizontal calendria respectively. The results show a marked increase in product concentration with increase in feed temperature. Feed liquor

TABLE 4.8

EFFECT OF FEED TEMPERATURE ON PERFORMANCE OF FORCED CIRCULATION EVAPORATOR (VERTICAL CALENDRIA)

Evaporator: L = 3m D = 5.03/5.43 cm n = 1 N=3

Process Conditions:

System: Bamboo Kraft Black Liquor

P_i = 181 kN/m^2 S_i = 45 per cent R_D = 0.17 m^2 K/kW

W_i = 2.5 kg/s D = 5.03/5.43 cm R = 3.5 T_s = 145^{o}C

T_i ^oC	μ cp	u m/s	N_{Re}	S_i percent	S_e per cent	S_o percent	ΔP kN/m^2	U_{nb} W/m^2 K	U_b W/m^2 K	U W/m^2 K
90.0	11.43	3.55	23235	48.43	-	49.13	105.64	1632	-	1632
100.0	11.66	3.68	21795	50.34	50.524	52.11	98.40	1636	2997	1696
110.0	12.66	4.08	16845	52.241	52.48	55.17	74.25	1631	3446	2215

TABLE 4.9

EFFECT OF FEED TEMPERATURE ON PERFORMANCE OF FORCED CIRCULATION EVAPORATOR (HORIZONTAL CALENDRIA)

Evaporator: L = 3m D = 5.03/5.43 cm n = 1 N=3

Process Conditions

System: Bamboo Kraft Black Liquor

P_i = 181 kN/m^2 S_i = 45 per cent W_i = 2.5 kg/s/Tube

R = 3.5 R_D = 0.17 m^2 K/kW

T_i ^oC	u m/s	μ cp	N_{Re}	S' percent	S_o per cent	U_{nb} W/m^2 K	ΔP kN/m^2
90.0	3.88	11.38	23349	48.24	49.15	1965	65.66
100.0	3.66	11.89	21316	50.55	52.35	1887	61.82
110.0	3.50	12.79	19096	52.78	55.53	1808	57.82

with an initial concentration of 45 per cent gives final product concentration range of 49 to 56 per cent, when temperrature of feed liquor changes from 90 to 110°C. For evaporator with horizontal calendria, most of the evaporation takes place in the separator and no boiling occurs inside calendria. Figure 4.13 shows a slight fall in overall heat transfer coefficient with increase in feed liquor temperature. This can be explained by the fact that, with increase in feed temperature concentration of mixed feed (fresh feed plus recycle liquor) increases and the resultant increase in viscosity lowers N_{Re}, and in turn causes a decrease in overall heat transfer coefficient. Figure 4.12 shows an increase in overall heat transfer coefficient with increase in feed liquor temperature. The latter increases the length of the boiling zone and gives a higher overall heat transfer coefficient.

4.3.2 Effect of Feed Liquor Concentration:

Feed liquor concentration is varied from 35 to 55 per cent, while keeping other parameters, feed temperature, recycle ratio, vacuum in the separator constant. Tables 4.10 and 4.11 summarises the simulation results for evaporator with vertical and horizontal calendria respectively. It is seen from the Tables 4.10 and 4.11 that overall heat transfer coefficient falls with increased concentration which raises the viscosity. Viscosity of liquor at 35 per cent concentration, increases from 4.8 cp, 100°C to 52 cp at 55 per cent concentration and

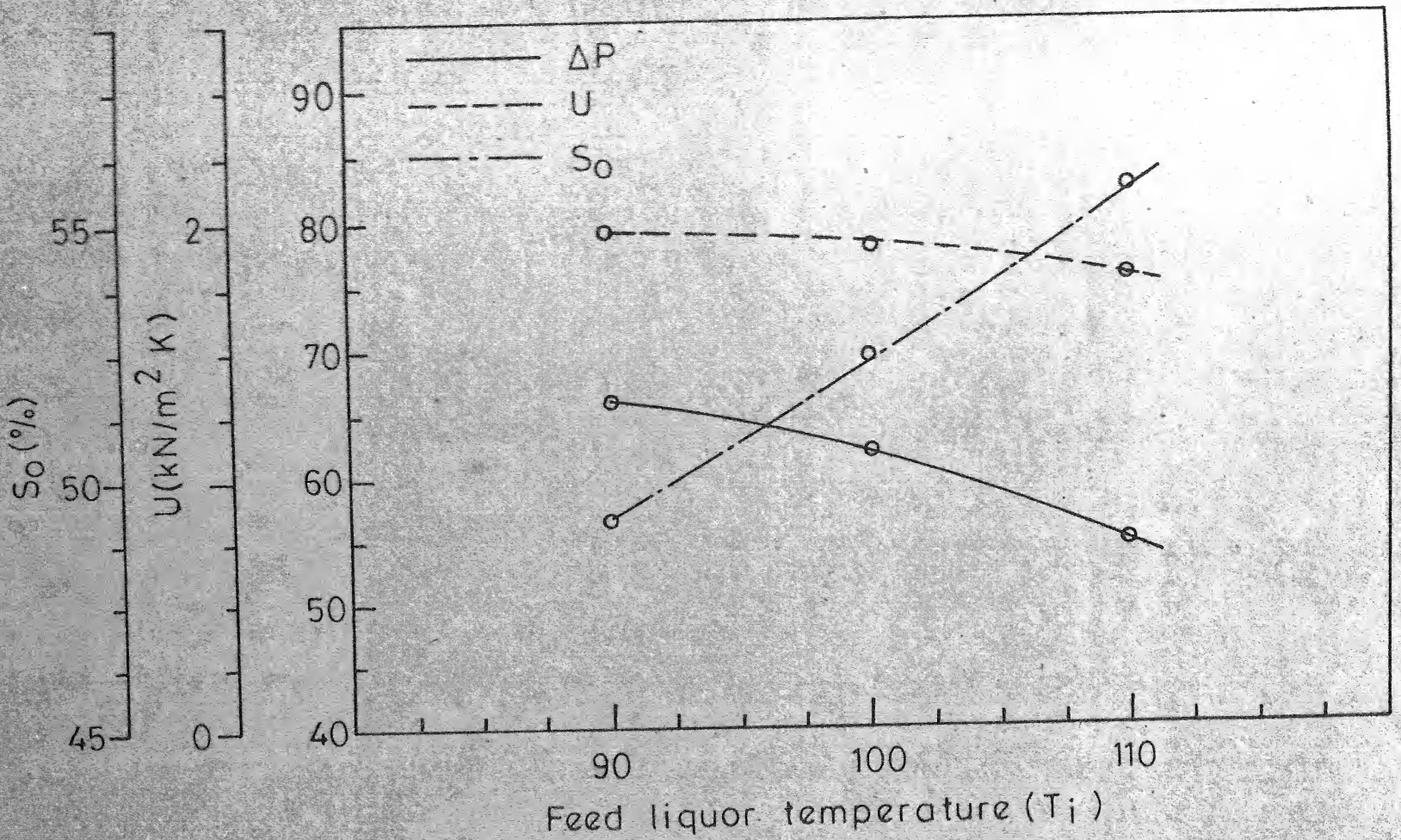

Fig. 4.13 - Effect of feed liquor temperature (Ti) on performance of FCE (horizontal calendria).

TABLE 4.10

EFFECT OF FEED LIQUOR CONCENTRATION ON PERFORMANCE OF FORCED CIRCULATION EVAPORATOR (VERTICAL CALENDRIA)

Evaporator: L = 3m D = 5.03/5.43 cm n = 1 N=3

Process Conditions:

System: Bamboo Kraft Black Liquor

P_i = 167 kN/m^2 T_i = 100^{o}C R = 3.5 T_s = 145^{o}C

R_D = 0.17 m^2 K/kW W_i = 2.5 kg/s/tube

S_i percent	u m/s	μ cp	N_{Re}	S' percent	S_e percent	S_o percent	ΔP kN/m^2	L_b m	U_{nb} W/m^2 K	U_b W/m^2 K	U W/m^2 K
35	3.83	4.86	52457	39.77	39.89	41.39	80.79	1.5	2784	5318	3206
40	3.76	5.44	43575	45.13	45.276	46.77	83.28	1.2	1901	3991	2179
45	3.68	11.50	21865	50.35	50.480	51.99	87.83	1.2	1640	3544	1893
50	3.63	23.84	10810	55.27	55.449	56.96	91.67	1.2	1406	2733	1583
55	3.62	50.00	5197	60.29	60.441	62.00	96.23	1.3	1134	2621	1348

TABLE 4.11

EFFECT OF FEED LIQUOR CONCENTRATION ON PERFORMANCE OF FORCED CIRCULATION EVAPORATOR (HORIZONTAL CALENDRIA)

Evaporator: L = 3m D = 5.03/5.43 cm n =1 N=3

Process Conditions:

System: Bamboo Kraft Black Liquor

P_i = 167 kN/m^2 T_i = 100^{o}C R = 3.5 W_i = 2.5 kg/s/tube

R_D = 0.17 m^2 K/kW T_s = 145^{o}C

S_i percent	u m/s	μ cp	N_{Re}	S' percent	S_o percent	ΔP kN/m^2 K	U W/m^2 K
35	3.83	4.83	52106	39.93	41.53	50.10	2275
40	3.73	5.63	46130	45.38	47.10	56.95	2284
45	3.66	11.95	21198	50.58	52.34	61.75	1884
50	3.63	23.84	10810	55.27	57.03	66.02	1564
55	3.64	51.97	4980	60.54	62.34	70.41	1235

100°C. For evaporator with vertical calendria boiling occurs in the tubes and the overall heat transfer coefficient is higher for all concentration than non-boiling heat transfer coefficient for evaporator with horizontal calendria. Figure 4.14 and Figure 4.15 show the overall performance based on Table 4.10 and 4.11. Total pressure drop increases with feed concentration and higher for evaporator with vertical calendria, due to the contribution of elevations head loss.

4.3.3 Effect of Recycle Ratio:

The rise in concentration of the liquor obtainable from a FCE unit with single pass of the liquor is usually small (less than 1.0 per cent), consequently the product is recycled to achieve a higher concentration of the final product. Simulation programme has been run to study the effect of recycle ratios of 1.5, 2.5, 3.5 and 4.5 on performance. Feed temperature and feed rate has been kept fixed. The effect of recycle ratio is shown by the results in Table 4.12 and 4.13 for FCE with vertical and horizontal calendria respectively. Figure 4.16 and 4.17 show that product concentration increases with increase in recycle ratio. Product concentration increases by 12 per cent for a three fold rise in recycle ratio. As recycle ratio is increased, more and more of concentrated product is being mixed with fresh feed, and as a result final product concentration increases. Total pressure drop

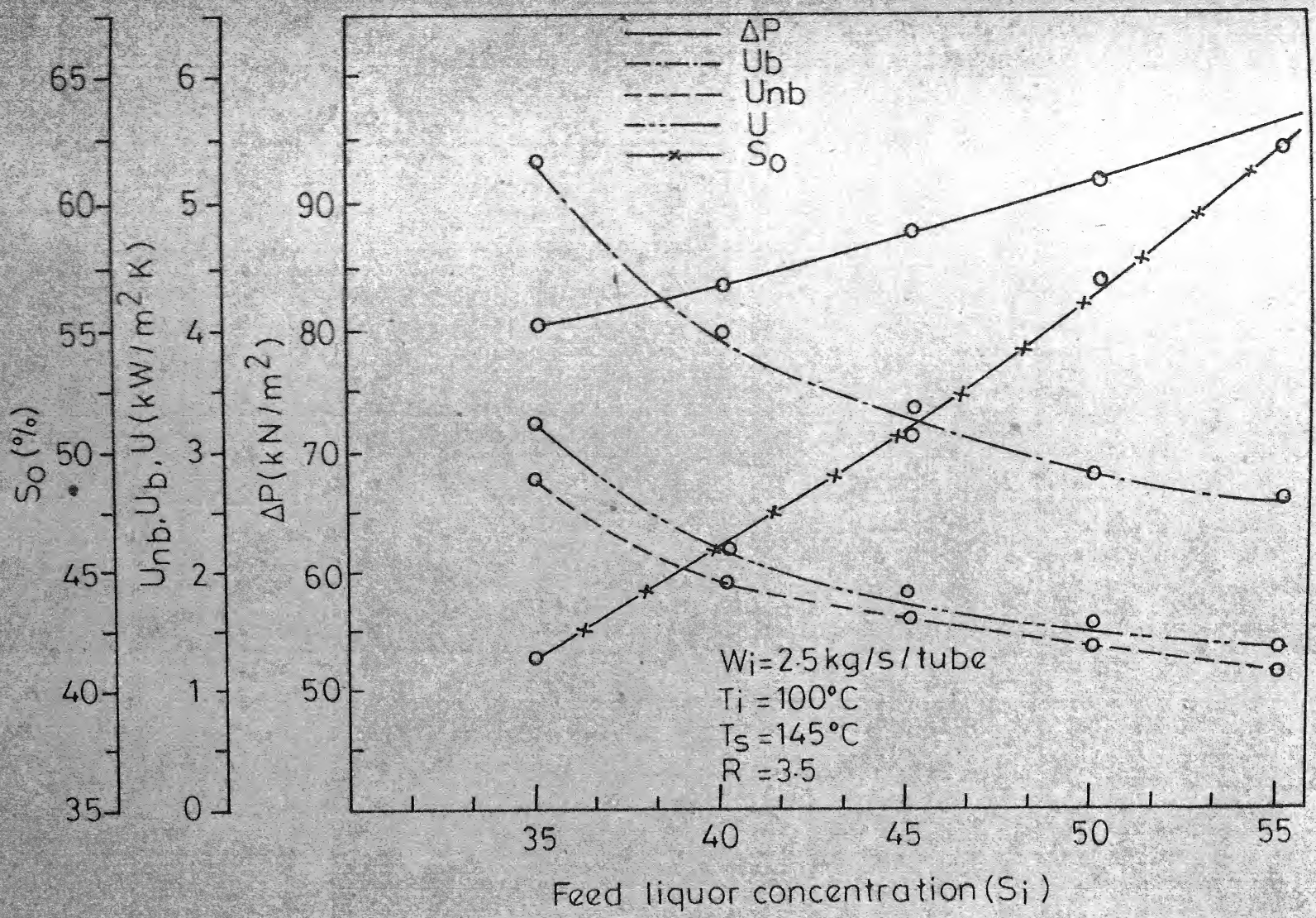

Fig. 4.14 - Effect of feed liquor concentration (Si) on performance of FCE (vertical calendria).

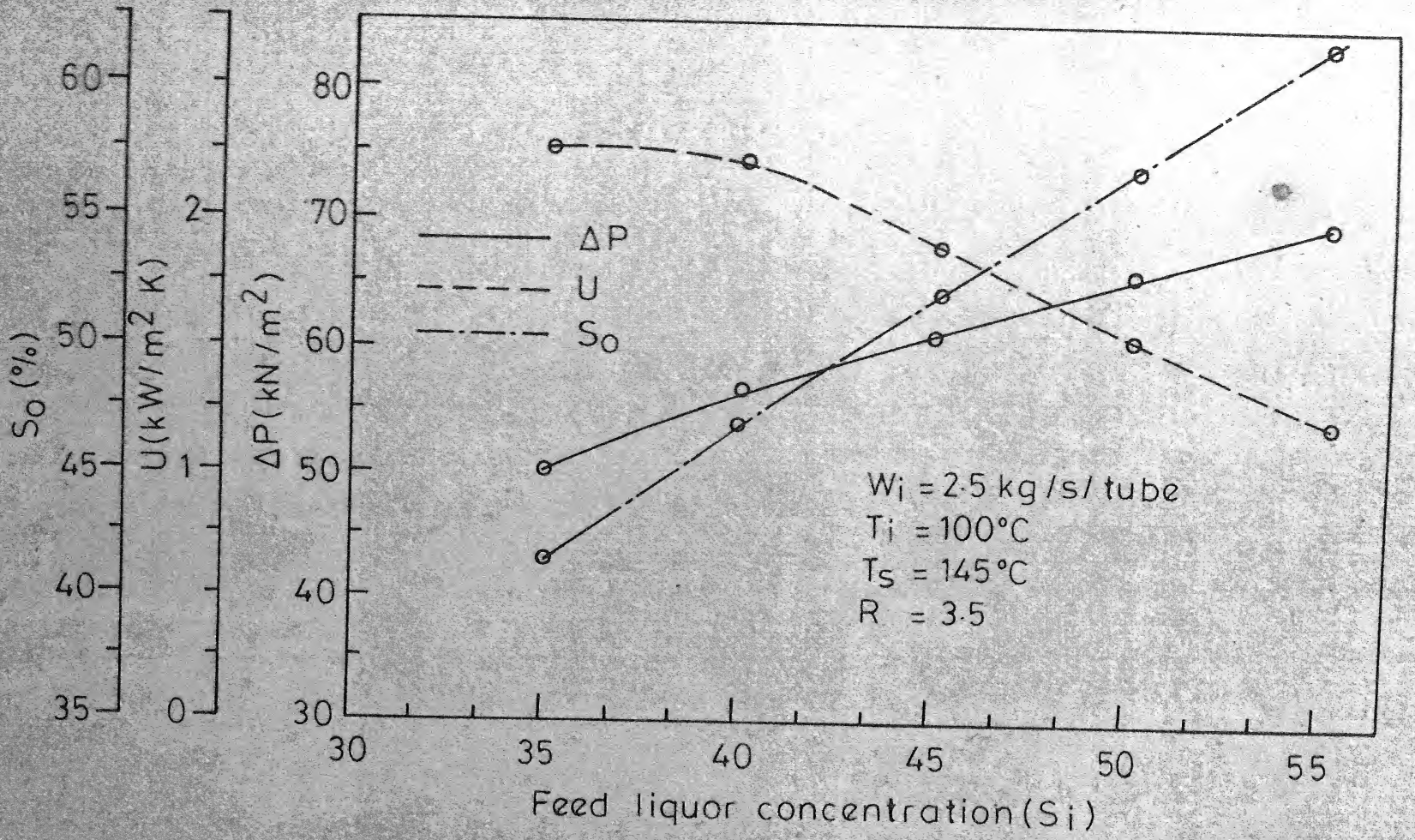

Fig. 4·15 - Effect of feed liquor concentration on performance of FCE (horizontal calendria).

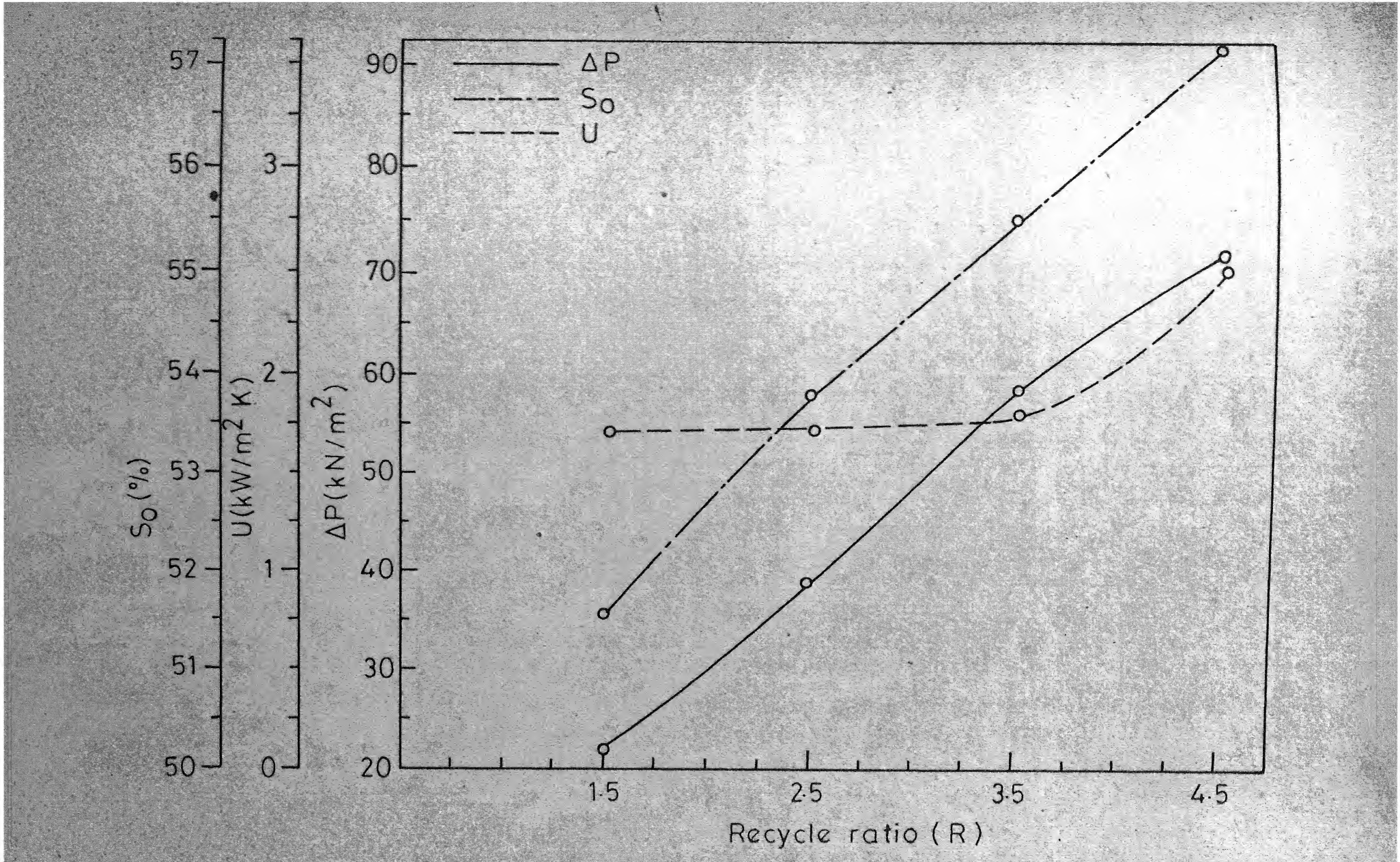

Fig. 4.17 - Effect of recycle ratio on performance of FCE(horizontal calendria).

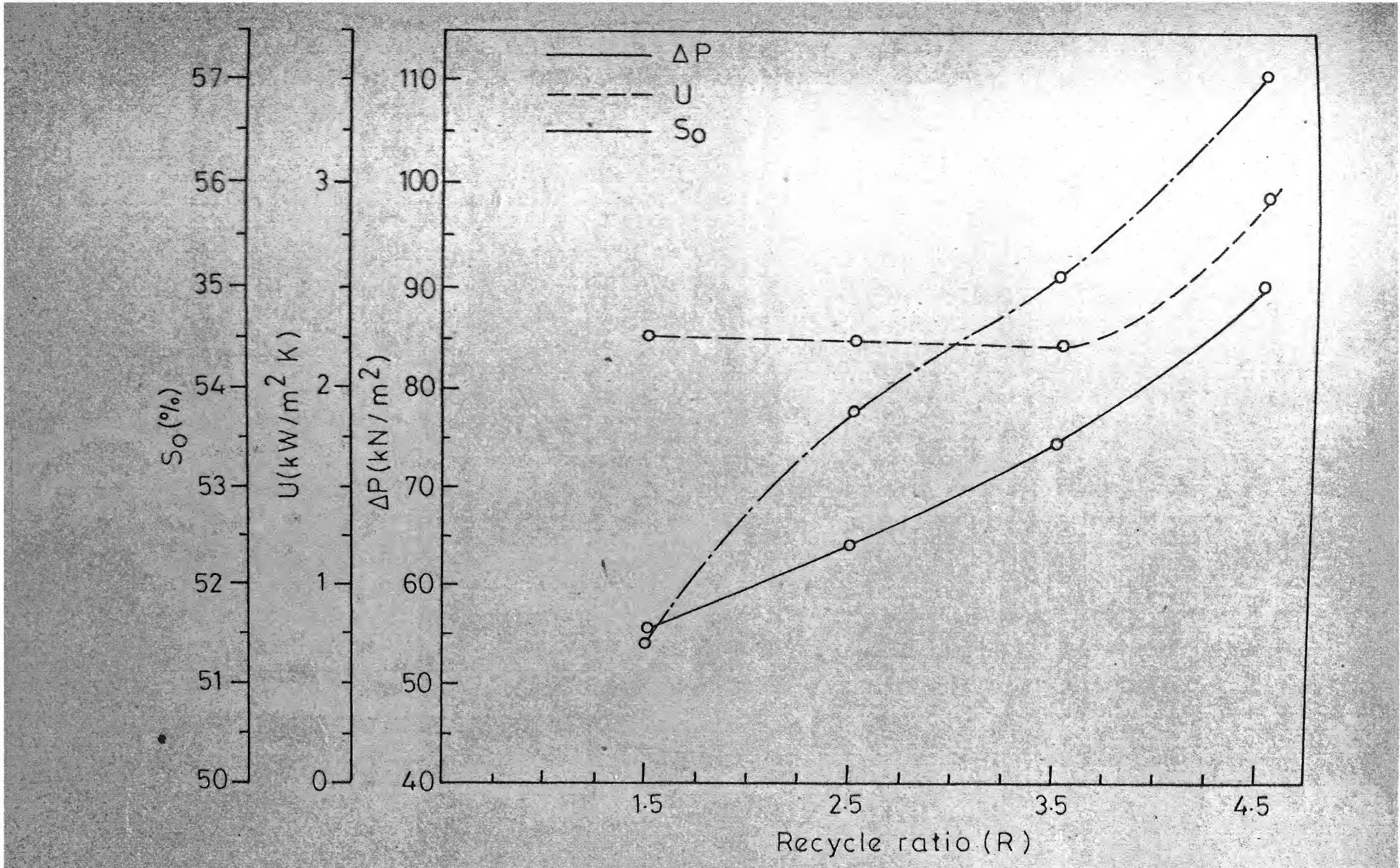

Fig. 4.16 - Effect of recycle ratio (R) on performance of FCE (vertical calendria).

TABLE 4.12

EFFECT OF RECYCLE RATIO ON PERFORMANCE OF FORCED CIRCULATION EVAPORATOR (VERTICAL CALENDRIA)

Evaporator: L = 3m D = 5.03/5.43 cm n = 1 N=3

Process Conditions:

System: Bamboo Kraft Black Liquor

$T_i = 110^oC$ $S_i = 45$ per cent $R_D = 0.17\ m^2\ K/kW$

$W_i = 2.5$ kg/s/tube $T_s = 145^oC$

P_i kN/m²	R	u m/s	μ cp	N_{Re}	S' percent	S_e percent	S_o percent	ΔP kN/m²	L_b m	U_{nb} W/m² K	U_b W/m² K	U W/m² K
182	1.5	2.14	6.96	21045	48.56	48.645	51.41	55.57	0.5	2190	3381	2260
182	2.5	2.82	10.33	18909	51.02	51.161	53.81	64.95	1.1	2187	3580	2241
182	3.5	3.50	12.79	19097	52.53	52.626	55.17	74.25	2.9	1631	3446	2215
196	4.5	4.09	16.87	17073	54.39	54.641	57.148	90.00	2.2	2260	3783	2980

TABLE 4.13

EFFECT OF RECYCLE RATIO ON PERFORMANCE OF FORCED CIRCULATION EVAPORATOR
(HORIZONTAL CALENDRIA)

Evaporator: L = 3m D = 5.03/5.43 cm n=1 N=3

Process Conditions:

System: Bamboo Kraft Black Liquor

P_i = 182 kN/m² R_D = 0.17 m² K/kW T_i = 110°C

S_i = 45 per cent W_i = 2.5 kg/s/tube T_s = 145°C

R	u m/s	μ cp	N_{Re}	S' percent	S_e percent	S_o percent	ΔP kN/m²	L_b m	U_{nb} W/m² K	U_b W/m² K	U W/m² K
1.5	2.14	7.20	20283	48.76	-	51.55	21.51	-	1739	-	1739
2.5	2.82	10.31	18947	51.01	-	53.79	38.20	-	1764	-	1764
3.5	3.48	13.12	18319	52.74	-	55.53	58.40	-	1808	-	1808
4.5	4.08	17.07	16845	54.47	54.554	57.20	71.04	2.9	1810	3042	2560

shows a rise with recycle ratio. From Table 4.13 it is observed that total pressure drop rise directly proportional with recycle ratio, while for vertical calendria this rise is about 65 per cent. This can be attributed to the fact in units with horizontal calendria pressure loss rises due to increase in end losses, which varies as the square of the liquid velocity inside the tube. As recycle ratio increases from 1.5 to 4.5, liquor velocity inside tube increases from 2.1 to 4.0 m/s. This rise in velocity greatly increases pressure loss at the ends. In evaporators with vertical calendria, though pressure loss increases with recycle, some pressure is recovered when liquor flows downward and more over boiling occurs inside tube for vertical orientation. Boiling inside tube and pressure recovery during downward flow contribute to the smaller rise in pressure loss.

Overall heat transfer coefficient does not change upto a recycle ratio of 3.5 beyond which it increases. Inspection of the values in Tables 4.12 and 4.13 shows a rise in average boiling heat transfer coefficient. Contributing towards improvement of overall heat transfer coefficient.

4.3.4 Effect of Feed Liquor Viscosity:

Effect of feed liquor viscosity was studied considering bamboo and bagasse black liquors. The viscosity for bagasse black liquor at 40 per cent concentration at 110°C is

TABLE 4.14

EFFECT OF VISCOSITY ON PERFORMANCE OF FORCED CIRCULATION EVAPORATOR(HORIZONTAL CALENDRIA)

Evaporator: L=3m, D=5.03/5.43 cm n = 1 N=3

Process Conditions

System: Bagasse Kraft Black Liquor

P_i = 186 kN/m^2 R_D=0.17 m^2 K/kW T_i = 110°C

S_i = 40 per cent W_i = 2.5 kg/s/tube

R	u m/s	μ cp	N_{Re}	S' per cent	S_o percent	U_{nb} W/m^2 K
2.5	2.45	15.57	10480	43.45	45.32	1543
4.5	3.53	20.06	11927	46.56	48.24	1700
6.5	4.48	29.97	10270	49.35	51.19	1650

8 cp. The recycle ratio was varied from 2.5 to 6.5. Results 12 cp and that for bamboo black liquor at 45 per cent and 110°C is 8 cp. The recycle ratio was varied from 2.5 to 6.5. Results for bagasse black liquor are summarised in Table 4.14. These results are compared with the values reported in Table 4.13, for bamboo black liquor with a feed concentration of 45 per cent for identical values of feed rate and temperature. These results show that overall heat transfer coefficient is smaller for bagasse black liquor compared to bamboo black liquor. At a recycle ratio of 2.5 the mixed feed concentrations are 43.5 and 51.0 per cent for bagasse and bamboo black liquors respectively, the corresponding viscosities are 15 and 10 cp at 110°C. The higher viscosity of bagasse black liquor lowers the overall heat transfer coefficient. At a recycle ratio of 4.5, the rise in final concentration is 12 and 8 per cent for bamboo and bagasse black liquors, respectively.

Table 4.14 shows a increase in overall heat transfer coefficient for bagasse black liquor from 1.54 to 1.70 kW/m^2 K, for recycle ratio upto 4.5, and decreases subsequently. N_{Re} increases from 10480 to 11920, due to increase in recycle ratio. Velocity of liquor velocity inside tube increases from 2.45 to 3.50 m/s, when recycle ratio is increased from 2.5 to 4.5. At the same time viscosity liquor entering the

the tube increases from 15.5 to 20.0 cp. At a recycle ratio of 6.5, though velocity increases to 4.5 m/s, viscosity of liquor entering the tube rises to 30 cp thereby lowering the values of N_{Re} and the overall heat transfer coefficient.

CHAPTER 5

SUMMARY

Mathematical model developed for steady state simulation of evaporation process in this work gives reliable prediction of its performance. The model was applied to Badger's experimental data and the results showed satisfactory agreement. The present model predicted boiling length and overall heat transfer coefficient in boiling zone within ±40 per cent and the agreement was within ±50 per cent for evaporation rate and total heat transferred in boiling zone. The model has been applied to simulate performance of evaporation in a single vertical tube operating on bamboo kraft black liquor. An increase in feed liquor concentration from 35 to 60 per cent decreased the overall heat transfer coefficient by 20 per cent. An increase in feed temperature (90-110°C) raised the overall heat transfer coefficient by 15 per cent. Two-fold increase in feed rate (5-10 kg/s/tube) gave a small increase (10 per cent) in overall heat transfer coefficient and pressure drop. Change in concentration of the feed liquor in a single pass unit was observed to be small (less than 1 per cent). The model was also used to study the performance of a forced circulation evaporator with recycle. Performance for evaporators with horizontal and vertical orientation of calendria was studied against variations of

REFERENCES

1 Anthony, E.D. and Robert, W.A., Chemical Engineering, March 23, 135 (1970).

2 Ibid, April 20, 151 (1970).

3 Ibid, May 4, 113 (1970).

4 Ibid, July 13, 95 (1970)

5 Ibid, August 10, 119 (1970).

6 Ibid, October 5, 87 (1970).

7 Ibid, November 2, 101 (1970).

8 Ibid, February 22, 125 (1971).

9. Agarwal, A.K., M.Tech. Thesis, I.I.T.,Kanpur, 1974.

10. Badger, W.L. and Brooks, C.H., Trans. Inst. Chem.Eng., 35, 392 (1937).

11 McNelly, M.J. and Coulson, J.M., Trans. Inst. Chem.Eng., 34, 247 (1956).

12 Dengler, C.E. and Addoms, J.N., Chem.Eng. Progr. Symp. Ser. No. 18, 52 (1956).

13 Anderson, G.H., and Mantzouranis, B.G., Chem.Eng. Science, 12, 109 (1960).

14. Penman, T.O. and Tait, R.W., Ind.Eng. Chem. Fundamentals, 4, 407 (1965).

15 Duckler, A.E., Moye Wicks, A.I.Ch.E.J., 10, 38-43 (Jan.1964).

16 Lockhart, R.W. and Martinelli, R.C., C.E.P., 45(1), 39(1949).

17 Harvin, R.L., Ph.D. Thesis, Univ. of Florida, 1955.

18 Orkiszewski, J. of Petroleum Technology, 829 (1967).

19 Gudmundson,C., Svensk Papperstindings, 75, 901 (1972).

20 Wallis, G.B., 'One Dimensional Two Phase Flow', McGraw Hill Book Co., New York (1969).

21 Tong, L.S., 'Boiling Heat Transfer and Two Phase Flow' R.E.K. Publishing Company, Huntington, New York (1975).

22 Martinelli, R.C. and Nelson, D.B.,'Recent Advances in Heat and Mass Transfer', McGraw Hill Book Co. New York (1961).

23 Bennet, J.A.R., Collier, J.G., Pratt, H.R.C., Trans. Inst. Chem. Engrs. (London) 39, 113-126 (1961).

24 Hewitt, G.F., Kearsey, H.A., Lacey, P.M.C., 'Burnout and Nucleation in Climbing film Flow', U.K. Report AERE-R 4374 (1963).

25 Levy, S., 'Steam Slip - Theoretical Prediction from Momentum Model', Trans. ASME, Ser. C, J. Heat Transfer 82, 113-124 (1960).

26 Muscettola, M., 'Two Phase Flow Pressure Drop', U.K. Report AEEW-R 284, Winfrith (1963).

27 Holland, C.D., Fundamentals and Modelling of Separation Processes, Prentice-Hall, Inc., N.J.

28 Hewitt, G.F., Kearsey, H.A., 'Burnout and Nucleation in Climbing Film Flow', U.K. Report AERE-R 4374 (1964).

29 Coulburn, A.P., Trans. Am.Inst. Chem.Engr. 29, 174 (1933).

30 Eubank, C.C. and Proctor, W.S., S.M. Thesis in Chemical Engineering, M.I.T. (1951).

31 Guerrieri, S.A. and Talty, R.D., Chem.Eng. Progr. Symp. Ser. No. 18, 52, 69 (1956).

32 Schrock, V.E., and Grossman, L.M., Nucl. Sci. Eng. 12, 474 (1962).

33 Wright, R.M., 'Downflow Forced Convection Boiling of Water in Heated Tubes', Univ. of California, Berkeley, August, 1961, Rept. UCRL 9744.

34 Chen, J.C., ASME Paper 63-HT-34 (1969).

35 Forster, H.K. and N.Zuber, A.I.Ch.E. J. 1, 531-535 (1955).

36 Ghalke, S.N., M.Tech.Thesis, IIT-Kanpur

37 Koorse, G.M., M.Tech. Thesis, IIT-Kanpur (Sept. 1972).

38 Perry, 'Chemical Engineering Handbook', McGraw Hill Book Company, Inc., New York (1963).

39 McCabe and Smith, 'Unit Operations', McGraw Hill Book Company, Inc., New York (1956).

40 Gesana, O.C., Lientz, J.R. and Badger, N.L., Trans. Am. Inst. Chem.Eng., 36, 759 (1940).

APPENDIX A

TWO PHASE FLOW PRESSURE DROP IN BOILING ZONE

Martinelli and Nelson [22] postulated that three factors contribute to the pressure drop resulting from the two-phase flow of boiling mixture; these factors include the effects of frictional forces, momentum changes and hydrostatic forces.

(a) Frictional Pressure Drop Gradient:

Lockhart-Martinelli [22, 9] have shown that two-phase flow behaviour can be considered under four general categories consisting of the following pairs of conditions:

1. Both liquid and vapor can be turbulent, l(t)-v(t)
2. Both liquid and vapor can be viscous, l(v) -v(v)
3. Liquid can be viscous and vapor turbulent l(v)-v(t)
4. Liquid can be turbulent and the vapor viscous l(t)-v(v)

Amongst these turbulent flow pattern of both liquid and vapor phases will be dominant during forced circulation. For this case Lockhart and Martinelli [22] have shown that for isothermal two-phase flow the frictional pressure drop can be calculated from equation (A-1).

$$\left(\frac{\Delta P}{\Delta L}\right)_{TPF} = \left(\frac{\Delta P}{\Delta L}\right)_g \phi^2_{gtt} \qquad \text{(A-1)}$$

$(\frac{\Delta P}{\Delta L})_{TPF}$ - Frictional Pressure drop gradient due to two-phase flow

$(\frac{\Delta P}{\Delta L})_{g}$ - Pressure drop gradient only vapor is flowing

ϕ_g - Experimentally determined parameter and is correlated by means of the dimensionless parameter X.

Alternatively, two-phase frictional pressure drop can also be obtained from equation (A-2)

$$(\frac{\Delta P}{\Delta L})_{TPF} = (\frac{\Delta P}{\Delta L})_{L} \quad \phi^2_{ltt} \qquad \text{(A-2)}$$

$(\frac{\Delta P}{\Delta L})_{l}$ - Frictional pressure drop gradient if only liquid is flowing

ϕ_l - Parameter related to dimensionless parameter X.

The relationship between ϕ_l and ϕ_g is given by equation (A-3)

$$\phi_{ltt} = \frac{\phi_{gtt}}{X_{tt}^{\frac{2-n}{2}}} \qquad \text{(A-3)}$$

The value of the index-n in equation (A-3) depends upon the flow mechanism.

Dimensionless correlation parameter X_{tt} obtained by dimensional analysis is given by equation (A-4)

$$X_{tt} = (\frac{\rho_g}{\rho_l})^{1/(2-n)} \quad (\frac{\mu_l}{\mu_g})^{n/(2-n)} \quad (\frac{W_L}{W_g}) \qquad \text{(A-4)}$$

The quality of vapor and liquid mixture is defined by equation (A-5)

$$x = \frac{W_g}{W_l + W_g} \qquad (A-5)$$

Equation (A-4) can be written in terms of x as equation (A-6)

$$X_{tt} = \left(\frac{\rho_g}{\rho_l}\right)^{1/(2-n)} \left(\frac{\mu_l}{\mu_g}\right)^{n/(2-n)} \left(\frac{1-x}{x}\right) \qquad (A-6)$$

Index 'n' has a value of 0.2-0.25 [21]. A value of 0.25 is used in the calculation.

Martinelli-Nelson have modified equation (A-2) to get the following equation (A-7).

$$\left(\frac{\Delta P}{\Delta L}\right)_{TPF} = \left(\frac{\Delta P}{\Delta L}\right)_{L_o} (1-x)^{1.75}\, \phi_{ltt}^2 \qquad (A-7)$$

Equation (A-7) was obtained as a result of empirically determined relationship between superficial liquid pressure drop (only liquid flow rate) and the actual liquid pressure drop (total flow rate as liquid).

$$\left(\frac{\Delta P}{\Delta L}\right)_{LPF} = \left(\frac{\Delta P}{\Delta L}\right)_{L_o} (1-x)^{1.75} \qquad (A-8)$$

where $\left(\frac{\Delta P}{\Delta L}\right)_{L_o}$ is the frictional pressure drop gradient for the flow of 100 per cent liquid.

The parameter ϕ_{ltt} has been correlated in terms of X_{tt} by Anthony and Robert [5].

$$\begin{aligned}\phi_{ltt} = \mathrm{Exp}[&1.44065 - 0.50445 \cdot \ln(X_{tt}) + 0.06212 \cdot (\ln(X_{tt}))^2 \\ &-0.00106 \cdot (\ln(X_{tt}))^3 - 0.00101 \cdot (\ln(X_{tt}))^4 \\ &+0.00003 \cdot (\ln(X_{tt}))^5 + 0.00002 \cdot (\ln(X_{tt}))^6]\end{aligned} \qquad (A-9)$$

(b) Acceleration Pressure Gradient:

The contribution of momentum changes of the fluids to the accelerative pressure drop dP_a can be written as

$$A \cdot dP_a = \text{Rate of change of momentum}$$

$$A \cdot dP_a = d\left(\frac{W_l u_l}{g_c} + \frac{W_g u_g}{g_c}\right) \qquad \text{(A-10)}$$

$$W_L = W_T(1-x)$$

$$W_g = W_T \cdot x$$

dP_a can be calculated if u_l and u_g, phase velocities are known. u_l and u_g can be calculated from the knowledge of void fraction 'α'.

$$u_l = \frac{W_T(1-x)}{A(1-\alpha)\rho_l}, \qquad u_g = \frac{W_T x}{A\,\alpha\,\rho_g}$$

Now substituting for W_L, W_g, u_l and u_g in equation (A-10) we get

$$dP_a = \frac{W_T^2}{A^2 g_c} d\left(\frac{(1-x)^2}{\rho_l(1-\alpha)} + \frac{x^2}{\alpha\,\rho_g}\right)$$

$$\left(\frac{dP}{dz}\right)_a = \frac{G_T^2}{g_c} d\left(\frac{(1-x)^2}{\rho_l(1-\alpha)} + \frac{x^2}{\alpha\,\rho_g}\right) \qquad \text{(A-11)}$$

Equation (A-11) is used to determine accelerative pressure drop gradient.

(c) Pressure Drop Gradient Due to Elevation:

Pressure drop gradient due to elevation can be determined from the equation:

$$\left(\frac{dp}{dz}\right)_{\text{elevation}} = \rho_{tp}\,\frac{g}{g_c} \qquad \text{(A-12)}$$

where ρ_{tp} - weighted average density of two phase flow mixture.

APPENDIX B

PRESSURE DROP DUE TO SUDDEN EXPANSION AND CONTRACTION

(a) Pressure drop due to sudden expansion of vapor-liquid mixture.

Tong [21] gives equation (B-1) for pressure drop due to sudden expansion for steam-water mixture.

$$P_2-P_1 = \frac{\rho_F u^2}{2g_c} \; 2\sigma\,(1-\sigma)\left[\frac{x^2}{\alpha}\frac{\rho_F}{\rho_v} + \frac{(1-x)^2}{(1-\alpha)}\right] \qquad \text{(B-1)}$$

where $\sigma = A_1/A_2$

Subscripts 1 and 2 refer to the positions before and after restriction, respectively. It is assumed that thermodynamic phase equilibrium exists before and after the restriction and that no phase change occurs.

(b) Pressure drop due to sudden expansion and contraction of single phase liquid.

$$\text{Expansion loss: } P_2-P_1 = \frac{\rho_F u_F^2}{2 g_c}(1-\sigma)^2 \qquad \text{(B-2)}$$

$$\text{Contraction loss: } P_2-P_1 = K_c \frac{\rho_F u_F^2}{2 g_c} \qquad \text{(B-3)}$$

K_c = contraction coefficient

$= 0.4\left(1 - \frac{1}{\sigma}\right)$ for turbulent flow.

APPENDIX C

ANTOINE EQUATION CONSTANTS FOR WATER

TABLE C-1

Temperature range, °C	Antoine Equation Constants		
	A	B	C
0-30	8.184254	1791.3	238.10
30-40	8.1393986	1762.262	236.29
40-50	8.0886767	1739.351	234.10
50-60	8.0464204	1715.429	232.14
60-70	8.0116295	1965.167	230.41
70-80	7.9845588	1678.948	228.97
80-90	7.9634288	1665.924	227.77
90-100	7.948396	1656.39	226.86
100-150	7.9186968	1636.909	224.92

$$\log_{10} P = A - \frac{B}{T + C}$$

T = Temperature, °C

P = Pressure, mm of Hg.

TABLE C-2

Pressure Range mm Hg	Antoine Equation Constants		
	A	B	C
5-30	8.184254	1791.3	238.1
30-35	8.1393886	1707.262	236.29
35-90	8.0886767	1739.351	234.10
90-150	8.0464202	1715.429	232.14
150-230	8.0116295	1695.167	230.41
230-340	7.9845538	1678.948	228.97
340-520	7.9634238	1665.924	227.77
520-760	7.948396	1656.39	226.86
760-1500	7.9136968	1636.909	224.92

$$T = \frac{B}{A - \log_{10} P} - C$$

T = Temperature, ^{o}C

P = Pressure mm of Hg

APPENDIX D

SHELL SIDE HEAT TRANSFER COEFFICIENT

The shell side heat transfer coefficient for the film wise condensation of steam can be determined from equation D-1 for long vertical tube.

$$h = 1.13 \left[\frac{k_f^3 \rho_F^2 g \Delta H}{L \mu_f (T_{sv} - T_s)} \right]^{0.25} \qquad \text{(D-1)}$$

Shell side heat transfer coefficient for filmwise condensation on horizontal tube can be determined from equation D-2.

$$h = \left[\frac{k_f^3 \rho_F^2 g \Delta H}{D_o \mu_f (T_{sv} - T_s)} \right]^{0.25} \qquad \text{(D-2)}$$

H = latent heat of condensation, BTU/lb

g = gravitational acceleration ft/hr^2

L = length of tube, ft

D_o = outside tube diameter, ft

μ_f = viscosity of condensate film, lb/ft-hr

T_{sv} = saturated vapor temperature, ^oF

T_s = surface temperature, ^oF

A 58350

CHE-1979-M-DAS-STE